Bulletin of the Geological Survey of Japan, vol. 69 (1), p. 1–30, 2018

Article

Evaluation of straightforward and rapid multi-element analyses of stream sediments for geochemical mapping in the remote islands of Japan — Seto Inland Sea region —

Atsuyuki Ohta[1,*]

Atsuyuki Ohta (2018) Evaluation of straightforward and rapid multi-element analyses of stream sediments for geochemical mapping in the remote islands of Japan — Seto Inland Sea region —. *Bull. Geol. Surv. Japan*, vol. 69 (1), p. 1–30, 7 figs, 7 tables.

Abstract: The straightforward and rapid determination of 53 elements in stream sediments using ICP-AES (inductively coupled plasma atomic emission spectrometry), ICP-MS (inductively coupled plasma mass spectrometry), and AAS (atomic absorption spectrometry) were evaluated for the geochemical mapping of isolated islands. Samples of 0.1 g were decomposed with HF, HNO_3, and $HClO_4$ at 125–145°C for 3 h to improve the determination of elements, including refractory minerals. The concentrations of rare earth elements (REEs), Nb, and Ta increased by 5–15% on average, and those of Zr and Hf increased by 30% on average. For arsenic determination, 0.1 g samples were digested using a mixed acid solution with an oxidizing reagent ($KMnO_4$) at 120°C for 20 min. Decomposition without using the oxidizing reagent and/or extended decomposition times has been shown to cause a decrease in As concentrations in geochemical reference materials. However, similar As concentrations in stream sediment samples were obtained irrespective of $KMnO_4$ addition and decomposition time. AAS was used to Hg measurement after thermal decomposition of about 50 mg samples without pre-treatment. The estimated concentrations of 53 elements in geochemical reference materials measured using ICP-AES, ICP-MS and AAS were agreement with the recommended values. Thus, it is concluded that the precision and accuracy of the rapid and straightforward analysis for geochemical mapping were satisfactory.

Geochemical features of stream sediments in the isolated islands of the Seto Inland Sea were strongly influenced by the parent lithology distributed in their watershed. Enrichments of Na_2O, Al_2O_3, K_2O, Be, Rb, Nb, REEs, Ta, Th and U were observed in sediments from isolated islands with widely underlain granitic rocks. In contrast, MgO, TiO_2, V, Cr, MnO, Fe_2O_3, Ni, and Co were abundant in sediments from Shodoshima Island where mafic volcanic rock had erupted. Extreme enrichments of Cu, Zn, As, Mo, Cd, Sn, Sb, Hg, Pb, and Bi were found in sediments influenced by mineral deposits and anthropogenic activity.

Keywords: stream sediment; geochemical map; isolated island; rapid and simple analysis; multi-element analysis; ICP-AES, ICP-MS, AAS

1. Introduction

The spatial distributions of elements, i.e., geochemical maps, have been used to elucidate the natural background of elements on the earth surface for environmental assessment or as an efficient way to explore mineral deposits (Howarth and Thornton, 1983; Weaver *et al.*, 1983; Webb *et al.*, 1978). For such purposes, geochemical maps have been extended to covering more territory or obtaining higher resolution over a narrow area. Cross-boundary and sub-continental-scale geochemical mapping has been conducted in European countries (De Vos *et al.*, 2006; Reimann *et al.*, 2003; Salminen *et al.*, 2005). High-resolution geochemical maps have been generated for limited areas to elucidate elemental contamination processes in urban areas (Cicchella *et al.*, 2008; Johnson and Ander, 2008; Thornton *et al.*, 2008).

The Geological Survey of Japan, National Institute of Advanced Industrial Science and Technology (AIST) has created unique comprehensive nationwide geochemical maps of both the main lands of Japan and its surrounding ocean area (Imai *et al.*, 2010; Imai *et al.*, 2004). Subsequently, higher-density geochemical mapping in the Kanto region, including Tokyo, the capital of Japan, was published in

[1] AIST, Geological Survey of Japan, Institute of Geology and Geoinformation

[*] Corresponding author: A. Ohta,Central 7,1-1-1 Higashi, Tsukuba, Ibaraki 305-8567, Japan. Email: a.ohta@aist.go.jp

2015 (Imai *et al.*, 2015). The mapping project intendeds to evaluate the highly-resolution maps of multi-elements for environmental assessment and examine the mass transfer process from an urban area to the adjacent coastal sea. Aside from this, geochemical mapping of the remote Japanese islands with higher density has also been ongoing. Stream sediments on remote islands have been sampled to interpret spatial distribution of elements in the island arc region (e.g., Ohta *et al.*, 2017). Although the areas of remote islands are small, they provide important geochemical data that are not available in the main land. For instance, Oki and Iki Islands are covered with alkaline volcanic rocks, which are narrowly or sporadically distributed in the main islands of Japan (Ohta *et al.*, 2015). Furthermore, the geochemical map would also provide fundamental information to conserve the ecosystem indigenous to each isolated island.

In this study, we focus on the geochemical data of stream sediments in the remote islands of the Seto Inland Sea. The terrestrial area surrounding the western Seto Inland Sea is mainly composed of late Cretaceous Hiroshima granitic rocks in the southwest Chugoku region and early to late Cretaceous Ryoke granitic rocks in the northern part of the Shikoku region. However, the Seto Inland Sea also covers this continuous spatial distribution pattern of elements related to the two granitic rocks across the Chugoku and Shikoku regions (Ohta *et al.*, 2017). In the eastern region, Cretaceous marine sedimentary rocks (Izumi Group) outcrop in southern Awajishima Island. There are a limited number of outcrops in the watersheds dominantly occupied by the Izumi Group because the rock is found narrowly in the Kinki, Chugoku, and Shikoku regions. Thus, the geochemical data from stream sediments in the remote islands of the Seto Inland Sea are important to elucidate the continuity of spatial distributions of elements related to granitic rocks and their geochemical influence on stream sediments.

Ohta *et al.* (2017) highlighted the extreme enrichment of rare earth elements (REEs), Nb, Ta, and Th in marine sediments of the Seto Inland Sea. Those elements are abundant in refractory minerals, such as zircon, sphene, and monazite. Some improvement in decomposition methodology is needed to more quantitatively elucidate the transport of these elements from land to sea. In addition, analytical equipment has been renewed or added newly in our laboratory. The analyses of As and Hg for terrestrial geochemical mapping were previously subcontracted to ALS Chemex of Vancouver in British Columbia (Imai *et al.*, 2004). However, the addition of an Hg analyzer facilitated Hg analysis for marine geochemical mapping (Imai, 2010). Recently, an inductively coupled plasma mass spectrometer (ICP-MS) equipped with a He collision cell was used for the determination of As in a highly-density geochemical mapping in the Kanto region (Imai *et al.*, 2015). Therefore, the purpose of this study is to 1) re-evaluate the multi-element analyses using geochemical reference materials and stream sediment samples collected from isolated islands, and 2) discuss the geochemical features of stream sediments in remote islands of the Seto Inland Sea.

2. Study area and samples

2.1 Geology

Fig. 1 depicts a seamless digital geological map of Japan at a 1:200,000 scale (Geological Survey of Japan, AIST (ed.), 2015). In the western region (Fig. 1(a)), late Cretaceous Hiroshima granitic rocks widely intrude in remote islands (Igi *et al.*, 1987). Ryoke granitic rocks intruded during early to late Cretaceous time and primarily outcrop in Yashirojima Island (Igi *et al.*, 1987; Miyazaki *et al.*, 2016). Late Cretaceous felsic volcanic intrusive rocks are found narrowly in Etajima Island, Kurahashijima Island, Kami-kamagarijima Island, Omishima Island, and Hakatajima Island (Matsuura *et al.*, 2002; Yamada *et al.*, 1986). Late Cretaceous rhyolite-dacitic rocks outcrop in the western region: Kami-kamagarijima Island, Osaki-kamijima Island, Osaki-shimojima Island, and partly in Yashirojima Island. Felsic volcanic rocks distributed in Yashirojima Island erupted during the Miocene age (Yamada *et al.*, 1986). Sandstone and a mélange matrix of Early to Middle Jurassic accretionary complex associated with Triassic chert block and Carboniferous to Permian limestone underlay in Etajima Island, Shimo-kamagarijima Island, Kami-kamagarijima Island, Osaki-kamijima Island, Osaki-shimojima Island, Omishima Island, Ikuchijima Island, In-noshima Island, and Mukaishima Island (Matsuura *et al.*, 2002; Yamada *et al.*, 1986). High-pressure typed Sambagawa and high-temperature type Ryoke metamorphic rocks are scarcely distributed in isolated islands of the Seto Inland Sea.

In the east region (Fig. 1(b)), late Cretaceous plutonic rocks, mainly composed of granite, are widely intruded in Shodoshima Island (Makimoto *et al.*, 1995). Miocene mafic volcanic rocks outcrop primarily in the central part and Jurassic accretionary complex sandstone is marginally distributed in the northwest part (Makimoto *et al.*, 1995). Awajishima Island contains Cretaceous Ryoke granitoids in its northern part (Kurimoto *et al.*, 1998; Makimoto *et al.*, 1995). Cretaceous marine sedimentary rocks (Izumi Group), which are composed mainly of sandstone, and partly of mudstone and conglomerate, are distributed in the southern part of Awajishima Island. The flat part of the northern Awajishima Island is primarily covered with Neogene sediments. The wide plain field in the southern part is covered by Pleistocene to Holocene sediments.

2.2 Samples

Fifty-eight stream sediment samples were collected from 15 islands in the Seto Inland Sea from 2010 to 2011 (Fig. 2). Details of sampling location information are summarized in Table 1. The longitude and latitude are provided in the Japanese Geodetic Datum 2000 (JGD2000). The mean sampling density is one sample per

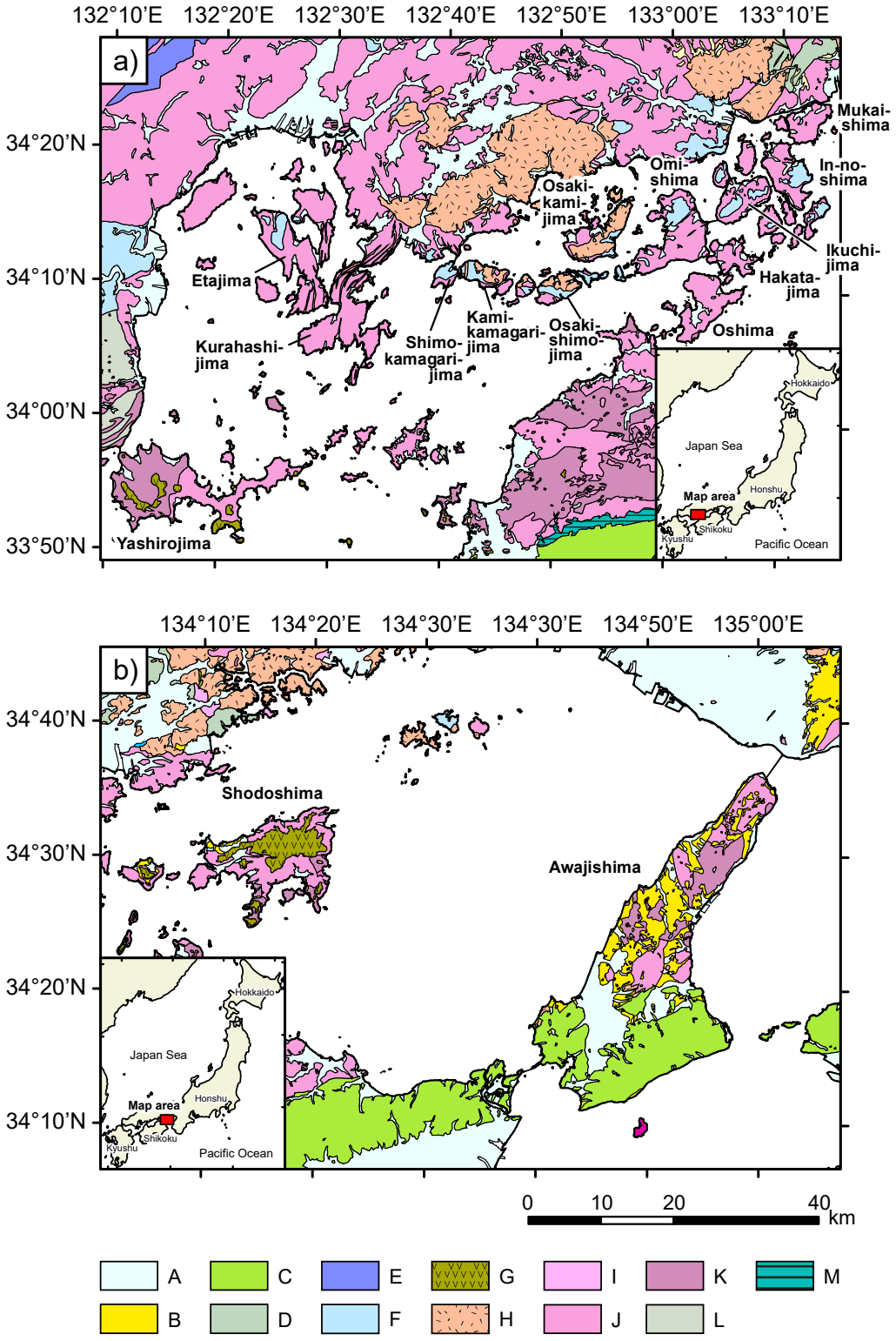

Fig. 1 Index map reffered from the Seamless Degital Geological map of Japan (1:200,000, Geological Survey of Japan, AIST (ed.), 2015). (a) The western region of the Seto Inland Sea. (b) The eastern region of the Seto Inland Sea. A: Quaternary sediments, B: Paleogene to Neogene sediments, C: Cretaceous sedimentary rocks, D: Permian sedimentary rocks, E: Sandstone and mélange matrix of Permian accretionary complex associated with exotic rocks, F: Sandstone and mélange matrix of Jurassic accretionary complex associated with exotic rocks, G: Miocene volcanic rocks (primarily mafic), H: Cretaceous rhyolite-dacitic rocks and felsic volcanic intrusive rocks, I: Paleogene granitic rocks, J: Late Cretaceous granitic rocks, K: Early to middle Cretaceous granitic rocks, L: Cretaceous high-temperature type metamorphic rocks, M: Cretaceous high-pressure type metamorphic rocks.

8–43 km^2, with a mean of 22 km^2, which is approximately fivefold the density of nationwide geochemical mapping (100–120 km^2). All rivers were maintained with revetment walls on both banks and the riverbed. In most cases, the width of the river was narrower than 20 m and the river depth shallower than 50 cm. However, some rivers in small isolated islands are just irrigation channels, so a small amount of sand had piled up. River water was not flowing in two rivers in Omishima Island on the sampling date. Stream sediments were collected from the river bed, dried at room temperature over two–three weeks and sieved through an 83 mesh (180 μm) screen. In addition, magnetic minerals were removed from the dried samples using a hand magnet to minimize the effect of magnetic mineral accumulation (Imai *et al.*, 2004).

The precision and accuracy of the analytical data for 53 elements were confirmed using the following 14 geochemical reference materials obtained from the Geological Survey of Japan: JSd-1, -2, -3, and -4 (stream sediments), JLk-1 (lake sediment), and JSl-1 and -2 (slate) (Imai *et al.*, 1996); JSO-1 (soil) and JMs-1 and -2 (marine sediments) (Terashima *et al.*, 2002a); JCFA-1 (coal fry ash) (Terashima *et al.*, 1998); JMn-1 (ferromanganese nodule) (Terashima *et al.*, 1995); JCu-1 (copper ore) (Okai *et al.*, 2002); and JZn-1 (zinc ore) (Okai *et al.*, 2002).

2. 3 Watershed analyses

The geochemistry of stream sediments is predominantly determined by the dominant lithology distributed in the water catchment area. To elucidate the dominant lithology distributed in the respective river systems, the watershed stream network was calculated based on a digital elevation model (50 m mesh data) obtained from the Geospatial Information Authority of Japan (GSI). The methodology followed Ohta *et al.* (2004) in all respects. Geographic information system software (ArcGIS 10.3; Environmental Systems Research Institute) was used for the calculation. Calculated watershed areas were 1.0–27 km^2, with a mean of 8.0 km^2.

We assumed that the elemental concentrations of stream sediments were determined by the representative lithology, which is the most widely distinctive rock type exposed in a drainage basin. The lithologies were Neogene and Quaternary unconsolidated sediments, Cretaceous sedimentary rocks, Cretaceous granitic rocks, Jurassic accretionary complexes comprise mainly of sandstone-mélange matrix, Cretaceous and Miocene felsic volcanic rocks, and Miocene mafic volcanic rocks. Table 2 summarizes the relative exposed areas of these lithologies in each drainage basin. Ryoke granitic rocks are the dominant lithology in the catchment area of Yashirojima Island. Hiroshima granitic rocks are the representative lithology for samples collected at Kurahashijima Island, Etajima Island, Ikuchijima Island, Oshima, and Omishima Island. Cretaceous felsic volcanic rocks are mainly distributed in the watershed of Osaki-kamijima Island and Kami-kamagarijima Island. Cretaceous granitic rocks and Miocene mafic volcanic rocks are the major lithologies in the watershed area of Shodoshima Island. Neogene-Quaternary sediments, Cretaceous sedimentary rocks, and Cretaceous granitic rocks are widely distributed in Awajishima Island. Neogene sediments are found only in Awajishima Island.

3. Analytical methods

All chemical reagents used in this study were Atomic Absorption Spectrometry (AAS) grade, and the potassium permanganate was an extra pure grade; all were obtained from Kanto Chemical Co. Inc. The moisture (H_2O^-) concentration of samples was determined with 0.2 g of stream sediment sample after drying at 110°C for 2 h. All concentration data were converted to a dry weight basis.

Each thermally dried sample, 0.1 g, was weighted in a 50 mL Teflon beaker with a Teflon watch glass. The sample was digested using 5 mL HF (50%), 3 mL HNO_3 (60–61%), and 2 mL $HClO_4$ (60–62%) at 125°C for 2 h and 145°C for 1 h. The digested product was evaporated to dryness at 190°C. The residue was dissolved in 5 mL of 7 mol/L HNO_3 at 100°C for 15 min. The dissolved solution was diluted to 100 mL in a polyethylene volumetric flask with double-deionized water. A solution of digested geochemical reference material JB-1a (Imai *et al.*, 1995) was used as a standard (Imai, 1990). A calibration line between the standard and blank solutions was provided. This method is easy and very effective to correct the matrix effect with major elements for multi-element analysis of igneous rocks (Imai, 1990). However, stream sediment samples generally have much higher concentrations of some elements, especially heavy metals, than igneous rocks due to high concentrations of clay minerals, inputs from ore-forming minerals and contamination discharge (Imai, 1987). Therefore, a high concentration standard solution was prepared from 1,000 mg/L standard solutions, obtained from Kanto Chemical Co. Inc., for elemental analyses of samples having more than tenfold higher concentrations of Li, Be, Cu, Zn, Cd, Mo, Sn, Sb, Cs, Tl, Pb, and Bi than those of JB-1a.

For As determination, 0.1 g of not thermally-dried samples were placed in Teflon vessels with a Teflon watch glass and digested using 2% m/m $KMnO_4$ solution (2 mL), 5 mL HF (50%), 2 mL HNO_3 (60–61%), and 1 mL $HClO_4$ (60–62%) at 120°C for 20 min, a procedure modified after Terashima (1976, 1984). The degraded product was evaporated at 190°C until the solution was <1 mL. After cooling, 10 mL of 6 mol/L HCl was added to the Teflon vessel with a Teflon watch glass and heated at 135°C for 30 min to reduce excess $KMnO_4$ and dissolve the degradation products. The HCl solution was finally diluted to 100 mL in a polyethylene volumetric flask with double-deionized water. A standard solution was prepared from a 1,000 mg/L arsenic atomic absorption standard solution (Kanto Chemical Co. Inc.). An acid solution was added to the standard solution equal to the concentrations

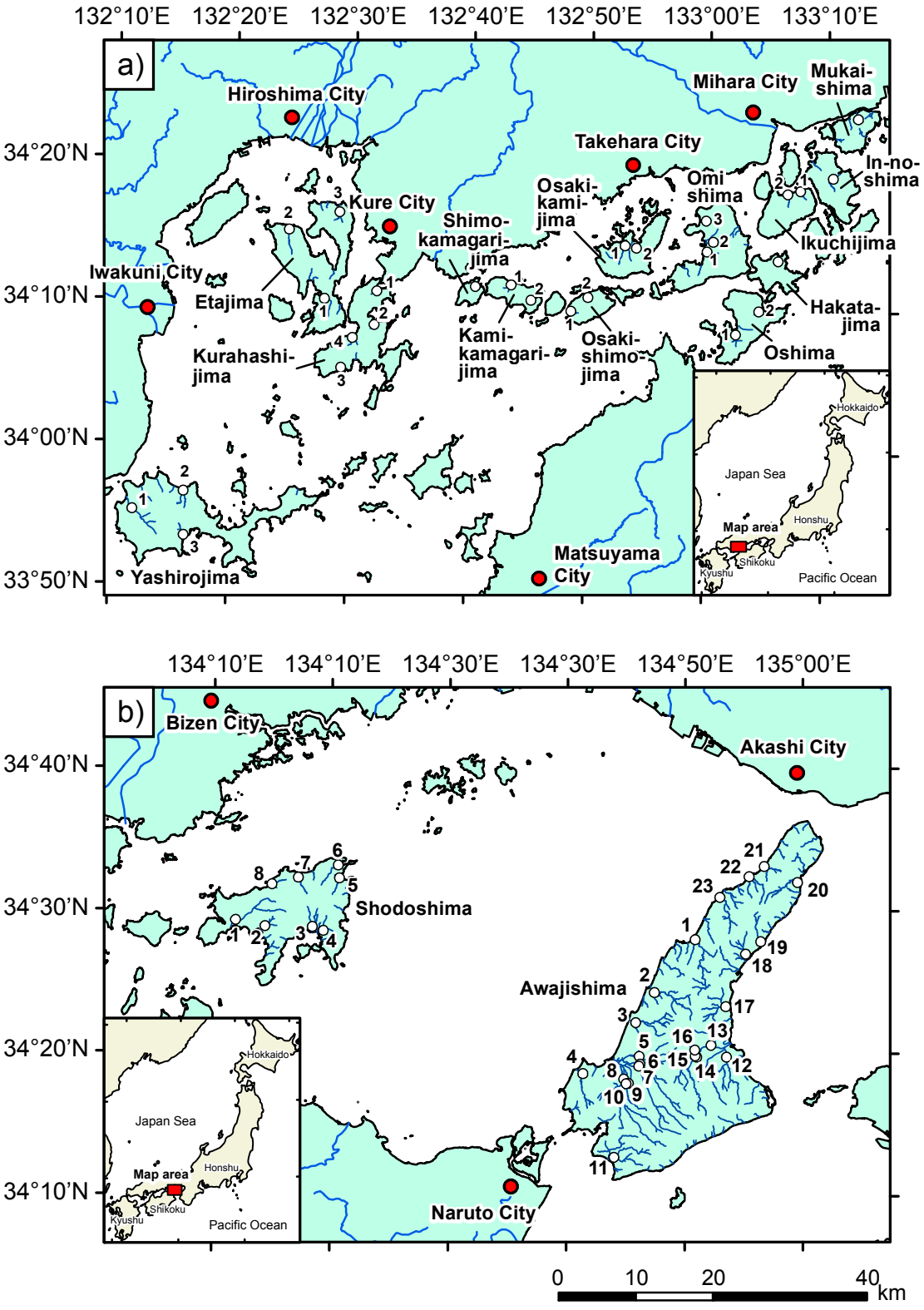

Fig. 2 Sampling locations of stream sediments in isolated islands of the western region (a) and the eastern region (b) of the Seto Inland Sea.

Table 1　Locations and descriptions of stream sediment samples and rivers.

Sample	Island		River		Longitude[a]	Latitude[a]	Sampling date	Width of rivers (m)	Depth of river (cm)	Flow rate of river
Ys1	Yashirojima	屋代島	Yashiro	屋代川	132°11'49.3"E	33°55'25.6"N	2010/11/30	10	20	very slow
Ys2	Yashirojima	屋代島	Tsuhara	津原川	132°16'5.8"E	33°56'46.2"N	2010/11/30	8	8	1m / 4s
Ys3	Yashirojima	屋代島	Miyakawa	宮川	132°16'10.4"E	33°53'38.9"N	2010/11/30	5	20	1m / 8s
Kr1	Kurahashijima	倉橋島	Ota	大田川	132°31'59.3"E	34°11'5.5"N	2010/12/1	10	5	1m / 4s
Kr2	Kurahashijima	倉橋島	Hase	長谷川	132°31'50.8"E	34°8'42.6"N	2010/12/1	1	5	1m / 5s
Kr3	Kurahashijima	倉橋島	Higashi-sugawa	東須川	132°29'5.8"E	34°5'40.4"N	2010/12/1	3	1	1m / 3s
Kr4	Kurahashijima	倉橋島	Otani	大谷川	132°29'59.7"E	34°7'47"N	2010/12/1	10	5	1m / 4s
Et1	Etajima	江田島	unknown	不明	132°27'35.3"E	34°10'29.1"N	2010/12/1	3	5	1m / 6s
Et2	Etajima	江田島	Kinoshita	木ノ下川	132°24'28.1"E	34°15'15.9"N	2010/12/1	4	30	1m / 15s
Et3	Etajima	江田島	Hase	長谷川	132°28'42"E	34°16'34.6"N	2010/12/1	7	4	1m / 7s
Ok1	Osaki-kamijima	大崎上島	Harada	原田川	132°52'52.5"E	34°14'38.5"N	2010/12/2	10	3	1m / 6s
Ok2	Osaki-kamijima	大崎上島	Harashita	原下川	132°53'51"E	34°14'29.6"N	2010/12/2	1	1	1m / 5s
Ok3	Osaki-shimojima	大崎下島	Kunihiro	国広川	132°48'23.4"E	34°9'58.2"N	2010/12/2	3	1	1m / 4s
Ok4	Osaki-shimojima	大崎下島	Takada	高田川	132°49'48.9"E	34°10'57.4"N	2010/12/2	4	1	1m / 3s
Km1	Shimo-kamagarijima	下蒲刈島	unknown	不明	132°40'18.2"E	34°11'33"N	2010/12/2	3	5	1m / 7s
Km2	Kami-kamagarijima	上蒲刈島	Tado-okawa	田戸大川	132°43'19.7"E	34°11'43.4"N	2010/12/2	1	1	n.d.
Km3	Kami-kamagarijima	上蒲刈島	Kajiya	梶屋川	132°45'0.4"E	34°10'40.2"N	2010/12/2	1	40	very slow
Ik1	Ikuchijima	生口島	Taisho	大正川	133°7'38"E	34°18'39.9"N	2010/12/3	3	5	1m / 3s
Ik2	Ikuchijima	生口島	Okita	沖田川	133°6'33.6"E	34°18'26.5"N	2010/12/3	1	10	1m / 3s
In1	In-noshima	因島	Okawa	大川	133°10'22.8"E	34°19'36"N	2010/12/3	4	2	1m / 3s
Mk1	Mukaishima	向島	unknown	不明	133°12'25"E	34°23'47.9"N	2010/12/3	3	5	1m / 10s
Os1	Oshima	大島	Moyai-okawa	舫大川	133°2'21.8"E	34°8'31.2"N	2010/12/3	0.5	40	1m / 6s
Os2	Oshima	大島	Okawa	大川	133°4'15.7"E	34°10'11.3"N	2010/12/3	12	40	1m / 2s
Ha1	Hakatajima	伯方島	Nakagawa	中川	133°5'50.9"E	34°13'43.7"N	2010/12/3	1	15	1m / 3s
Om1	Omishima	大三島	Utena-hongawa	台本川	132°59'49"E	34°14'19.6"N	2010/12/3	no flow	no flow	n.d.
Om2	Omishima	大三島	Miyaura-honkawa	宮浦本川	133°0'19.8"E	34°15'1.7"N	2010/12/3	no flow	no flow	n.d.
Om3	Omishima	大三島	Kochi	高知川	132°59'42.3"E	34°16'29.1"N	2010/12/3	3	1	1m / 3s
Sd1	Shodoshima	小豆島	Denpo	伝法川	134°11'44.4"E	34°29'28.6"N	2011/11/29	20	5	1m / 4s
Sd2	Shodoshima	小豆島	Ikeda-okawa	池田大川	134°14'14.1"E	34°29'3.4"N	2011/11/29	10	25	very slow
Sd3	Shodoshima	小豆島	Betto	別当川	134°18'13.7"E	34°29'1"N	2011/11/29	5	20	1m / 3s
Sd4	Shodoshima	小豆島	Yasuda-okawa	安田大川	134°19'10.1"E	34°28'45.1"N	2011/11/29	4	30	1m / 13s
Sd5	Shodoshima	小豆島	Morisho	森庄川	134°20'29.9"E	34°32'25.8"N	2011/11/29	15	20	very slow
Sd6	Shodoshima	小豆島	Yoshida	吉田川	134°20'23.7"E	34°33'20.3"N	2011/11/29	10	10	very slow
Sd7	Shodoshima	小豆島	Katsura	桂川	134°17'1.8"E	34°32'28.7"N	2011/11/29	15	N.D.	very slow
Sd8	Shodoshima	小豆島	Tachibana	橘川	134°14'48.1"E	34°31'59.7"N	2011/11/29	10	15	1m / 16s
Aw1	Awajishima	淡路島	Gunge	郡家川	134°50'43.6"E	34°28'12"N	2011/11/30	30	70	1m / 13
Aw2	Awajishima	淡路島	Tsushi	郡志川	134°47'15.5"E	34°24'28.5"N	2011/11/30	7	10	1m / 4s
Aw3	Awajishima	淡路島	Torikai	鳥飼川	134°45'40.4"E	34°22'22.3"N	2011/11/30	5	13	1m / 5s
Aw4	Awajishima	淡路島	Tsui	津井川	134°41'14.3"E	34°18'46.5"N	2011/11/30	7	10	n.d.
Aw5	Awajishima	淡路島	Shito-ori	倭文川	134°45'58.9"E	34°19'59.6"N	2011/11/30	30	60	very slow
Aw6	Awajishima	淡路島	Nariai	成相川	134°46'4.4"E	34°19'26.9"N	2011/11/30	7	15	1m / 6s,
Aw7	Awajishima	淡路島	Mihara	三原川	134°45'56.6"E	34°19'19.4"N	2011/11/30	3	50	1m / 3s
Aw8	Awajishima	淡路島	Shinkawa	新川	134°44'40.9"E	34°18'24.1"N	2011/11/30	3	40	1m / 4s
Aw9	Awajishima	淡路島	Umanorisute	馬乗捨川	134°45'3.7"E	34°18'5.3"N	2011/11/30	10	30	1m / 18s
Aw10	Awajishima	淡路島	Dainiti	大日川	134°44'51.6"E	34°18'4.1"N	2011/11/30	20	N.D.	very slow
Aw11	Awajishima	淡路島	Honjo	本庄川	134°43'51.1"E	34°12'54.8"N	2011/11/30	10	20	very slow
Aw12	Awajishima	淡路島	Chikusa	千草川	134°53'22.3"E	34°19'57.8"N	2011/12/1	15	10	n.d.
Aw13	Awajishima	淡路島	Sumoto	洲本川	134°52'2.3"E	34°20'46.5"N	2011/12/1	20	5	1m / 4s
Aw14	Awajishima	淡路島	Ayuya	鮎屋川	134°50'52"E	34°19'57.7"N	2011/12/1	3	15	1m / 3s
Aw15	Awajishima	淡路島	Hatsuo	初尾川	134°50'44.7"E	34°20'1.7"N	2011/12/1	4	15	1m / 10s
Aw16	Awajishima	淡路島	Sumoto	洲本川	134°50'42.2"E	34°20'27.4"N	2011/12/1	5	20	1m / 5s
Aw17	Awajishima	淡路島	Iwato	岩戸川	134°53'19.2"E	34°23'29.4"N	2011/12/1	20	>70	1m / 8s
Aw18	Awajishima	淡路島	Ikuho	生穂川	134°54'58.9"E	34°27'10.5"N	2011/12/1	4	5	1m / 6s
Aw19	Awajishima	淡路島	Sano	佐野川	134°56'16.3"E	34°28'3.4"N	2011/12/1	4	10	1m / 3s
Aw20	Awajishima	淡路島	Urakawa	浦川	134°59'22.8"E	34°32'13.6"N	2011/12/1	4	10	1m / 3s
Aw21	Awajishima	淡路島	Nojima	野島川	134°56'32.4"E	34°33'20.7"N	2011/12/1	2	25	1m / 4s
Aw22	Awajishima	淡路島	Tomishima	富島川	134°55'18.1"E	34°32'37.5"N	2011/12/1	3	15	1m / 5s
Aw23	Awajishima	淡路島	Murotsu	室津川	134°52'48.6"E	34°31'10.8"N	2011/12/1	12	20	1m / 4s

[a]JGD2000

Table 2 Area of watershed and estimated ratios of exposed area of lithologies distributed in each watershed.

Sample	Watershed area (km^2)	N-Qs	Cs	ACC	Fv	Mv	Gr	Oth	Dominant lithology
Ys1	14.4	1%	0%	0%	21%	0%	78%	0%	Gr
Ys2	4.9	3%	0%	0%	29%	0%	69%	0%	Gr
Ys3	5.0	0%	0%	0%	31%	0%	69%	0%	Gr
Kr1	2.2	6%	0%	0%	0%	0%	94%	0%	Gr
Kr2	2.7	0%	0%	0%	0%	0%	100%	0%	Gr
Kr3	1.0	0%	0%	0%	0%	0%	100%	0%	Gr
Kr4	3.0	8%	0%	0%	0%	0%	92%	0%	Gr
Et1	2.5	13%	0%	0%	0%	0%	87%	0%	Gr
Et2	6.1	7%	0%	67%	0%	0%	25%	0%	ACC
Et3	2.6	1%	0%	0%	0%	0%	99%	0%	Gr
Ok1	3.0	7%	0%	0%	56%	0%	37%	0%	Fv
Ok2	1.2	8%	0%	32%	60%	0%	0%	0%	Fv
Ok3	1.6	8%	0%	46%	0%	0%	46%	0%	ACC and Gr
Ok4	1.8	7%	0%	55%	37%	0%	0%	0%	ACC
Km1	1.6	3%	0%	90%	0%	0%	7%	0%	ACC
Km2	1.8	0%	0%	39%	61%	0%	0%	0%	Fv
Km3	1.0	10%	0%	0%	54%	0%	37%	0%	Fv
Ik1	2.9	5%	0%	37%	0%	0%	58%	0%	Gr
Ik2	2.5	3%	0%	27%	0%	0%	69%	0%	Gr
In1	4.2	10%	0%	47%	0%	0%	43%	0%	ACC and Gr
Mk1	2.6	0%	0%	2%	0%	0%	98%	0%	Gr
Os1	4.7	30%	0%	0%	0%	0%	70%	0%	Gr
Os2	2.9	1%	0%	0%	0%	0%	95%	4%	Gr
Ha1	2.1	16%	0%	0%	0%	0%	84%	0%	Gr
Om1	7.9	5%	0%	0%	0%	0%	94%	1%	Gr
Om2	2.3	5%	0%	11%	0%	0%	84%	0%	Gr
Om3	2.6	9%	0%	84%	0%	0%	7%	0%	ACC
Sd1	17.9	18%	0%	2%	0%	55%	24%	1%	Mv
Sd2	4.6	3%	0%	0%	0%	17%	80%	0%	Gr
Sd3	8.6	3%	0%	0%	1%	53%	43%	0%	Mv
Sd4	6.4	5%	0%	0%	1%	22%	70%	3%	Gr
Sd5	3.7	0%	0%	0%	0%	74%	26%	0%	Mv
Sd6	5.9	1%	0%	0%	0%	64%	35%	0%	Mv
Sd7	4.8	1%	0%	0%	0%	81%	18%	0%	Mv
Sd8	5.6	2%	0%	0%	0%	71%	27%	0%	Mv
Aw1	24.5	78%	0%	0%	0%	0%	22%	0%	Sed
Aw2	19.6	44%	0%	0%	0%	0%	55%	1%	Gr
Aw3	17.0	75%	0%	0%	0%	0%	23%	2%	Sed
Aw4	11.1	8%	91%	0%	0%	0%	0%	1%	Cs
Aw5	15.4	64%	13%	0%	12%	0%	9%	2%	N-Qs
Aw6	16.8	31%	67%	0%	0%	0%	0%	3%	Cs
Aw7	21.0	39%	59%	0%	0%	0%	0%	2%	Cs
Aw8	7.3	20%	79%	0%	0%	0%	0%	1%	Cs
Aw9	8.2	77%	19%	0%	0%	0%	0%	4%	N-Qs
Aw10	27.3	38%	60%	0%	0%	0%	0%	1%	Cs
Aw11	12.7	8%	92%	0%	0%	0%	0%	0%	Cs
Aw12	24.8	10%	89%	0%	0%	0%	0%	1%	Cs
Aw13	6.5	77%	9%	0%	0%	0%	13%	0%	N-Qs
Aw14	12.0	28%	69%	0%	0%	0%	0%	3%	Cs
Aw15	14.7	30%	66%	0%	1%	0%	2%	1%	Cs
Aw16	5.8	7%	1%	0%	0%	0%	92%	0%	Gr
Aw17	17.2	55%	0%	0%	0%	0%	44%	1%	N-Qs
Aw18	7.3	22%	0%	0%	0%	0%	77%	1%	Gr
Aw19	6.5	4%	0%	0%	0%	0%	96%	0%	Gr
Aw20	11.1	25%	0%	0%	0%	0%	73%	1%	Gr
Aw21	6.8	39%	0%	0%	0%	0%	59%	3%	Gr
Aw22	7.2	29%	0%	0%	0%	0%	70%	1%	Gr
Aw23	13.0	43%	0%	0%	0%	0%	57%	0%	Gr

N-Qs: Neogene-Quaternary sediments, Cs: Cretaceous sedimentary rocks (Izumi Group), ACC: Jurassic accretionary complexes (mainly sedimentary rocks), Fv: Miocene or Cretaceous felsic volcanic rocks, Mv: Miocene mafic volcanic rocks, Gr: Cretaceous granitic rocks, Oth: other rocks.

of matrix reagents in the sample solution. To evaluate the decomposition method for As, geochemical reference materials were also decomposed with or without using the $KMnO_4$ solution and digested samples at the different decomposition temperature and time.

Concentrations of 52 elements in stream sediments were determined using ICP-AES and ICP-MS using the calibration-curve method. To determine Na, Mg, Al, P, K, Ca, Sc, V, Ti, Cr, Mn, Fe, Co, Ni, Cu, Zn, Sr, Y, Zr, Sn, Ba, and Pb, a simultaneous echelle type ICP-AES (Thermo Fisher Scientific, iCap 6300) was used. Concentrations of each element were determined using multiple wavelengths and different plasma view configurations (axial or radial plasma viewing). The respective wavelengths and plasma view configurations chosen for the final determination are provided in Table 3. The radial view configuration was primarily employed to determine major elements, and the axial view configuration, with high sensitivity, was employed to measure Ti, Mn, P, Li, Be, Sc, V, Cr, Ni, Cu, Zn, Sr, Y, Zr, Sn, Ba, and Pb. A standard solution was inserted for measurement every five samples to correct for drift in signal intensity. A solution of digested geochemical reference material JB-3 (Imai *et al.*, 1995) was measured every ten samples for quality control. The internal standard method was not applied to ICP-AES measurement. Major elements, Na, Mg, Al, P, K, Ca, Ti, Mn, and Fe, in sediments are expressed as oxides because they are most abundant in the Earth's crust and their abundance is frequently expressed in terms of weight percent oxide (Ohta *et al.*, 2010).

An ICP-MS (Agilent Technologies Inc. 7500ce) equipped with a He collision cell was used to determine the minor elements (Li, Be, Sc, Cr, Co, Ni, Cu, Zn, Ga, As, Rb, Y, Zr, Nb, Mo, Cd, Sn, Sb, Cs, La, Ce, Pr, Nd, Sm, Eu, Gd, Tb, Dy, Ho, Er, Tm, Yb, Lu, Hf, Ta, Tl, Pb, Bi, Th, and U). The respective masses chosen for determination are provided in Table 3. The blank, standard, and sample solutions were mixed with a 100 μg/L indium solution and diluted tenfold with doubly ionized water using an automatic dilution system. The solution was diluted to twenty-fold with doubly ionized water for arsenic determination. The dilution rate of the sample solution was corrected using the signal intensity for ^{115}In. The standard solution was measured every five samples to correct the drift in signal intensity. The solution of digested geochemical reference material JB-3 was measured every ten samples for quality control for all the elements except As. The solution of digested geochemical reference material JSl-1 was used for quality control of As determination.

The Hg concentrations in the stream sediments were determined using an atomic absorption spectrometer (AAS) that measured the quantity of Hg vapor generated from direct thermal decomposition of samples (Nihon Instruments Corp.; MA-2000). A standard solution prepared from a 1000 mg/L mercury atomic absorption standard solution (Kanto Chemical Co. Inc.) was used to provide the calibration-curve. Not thermally dried samples, 30–60 mg, and 50–200 mL of standard solutions were heated to volatilize Hg in samples. Mercury vapor was trapped as gold amalgam to reduce interference from elements such as halogen. Then, mercury vapor produced in the second heating process was measured with the AAS using wavenumber 253.7 nm. Geochemical reference materials JSl-1, JSl-2, and JLk-1 were used to correct the drift in signal intensity in response to Hg concentrations in samples.

4. Results and discussion

4. 1 Precision and accuracy of geochemical reference material measurements determined by ICP-AES and ICP-MS

Table 4 summarizes the four repeated analyses for 52 elements in Japanese stream sediment reference materials determined by ICP-AES and ICP-MS. The estimated concentrations and repeatability errors (the standard deviation (SD) of 1) of elements were comparable to the certified and recommended values. The estimated recovery rates for samples primarily ranged from 95% to 105% of the bulk compositions. The elemental concentrations of Li, Be, Sc, Cr, Co, Ni, Cu, Zn, Zr, Y, Sn, and Pb determined by ICP-AES and ICP-MS were crosschecked. The data were mutually consistent: the concentration ratios of these elements, except for Co, determined by ICP-AES and ICP-MS were 0.95-1.05 (Table 4a and 4b). The recovery rates of Zr (15–88%) and Hf (19–37%) in geochemical reference materials were quite low because the heavy mineral fraction, including zircon ($ZrSiO_4$), cannot be completely decomposed with the three-acid (HF, HNO_3, and $HClO_4$) digestion. The incomplete decomposition of these minerals also affects the measured concentrations of Nb, Ta, HREE, Th, and U. The concentrations of Nb, Ho, Yb, Lu, Ta, Th and U in JSd-2 and JSd-3 were 10–28% lower than the reference values (Table 4b). However, the incomplete decomposition of refractory minerals was a less serious problem for these elements compared to Zr and Hf.

When JB-1a was used as the standard to determine high concentrations of Li, Be, Cu, Zn, Cd, Mo, Sn, Sb, Cs, Tl, Pb, and Bi, the concentrations of Li, Cu, and Mo were 1.1–1.2 times higher; Zn, Sn and Tl were 1.0–1.1 times higher; Pb was 1.1–1.3 times higher; Bi was 1.0–1.1 times lower; and Cd was 1.5–2.0 times lower than the corresponding elements determined using a high concentration standard solution. For Be, Sb, and Cs measurements, there were no significant differences between the two standard solutions. These results suggest that a high concentration standard solution is necessary complement a reference rock standard solution, in this case JB-1a, to analyze Cd and Pb and is also preferable for Li, Cu, and Mo for geochemical mapping.

The relative standard deviations (RSDs) for the major elements, except Al_2O_3, were < 2% for major elements, 2–5% for Al_2O_3, and 1–5% for minor elements. The RSDs

Table 3 Wavelengths and plasma view configurations used for ICP-AES analysis and mass for ICP-MS.

iCap 6300 ICP-AES			7500ce ICP-MS	
Element	Wavelength (nm)	Plasma view	Element	Mass
Major elements			Li	7
Na	589.592 (I)	Radial	Be	9
Mg	202.582 (I)	Radial	Sc	45
Al	237.312 (I)	Axial	Cr	53
P	213.618 (I)	Axial	Co	59
K	766.490 (I)	Radial	Ni	60
Ca	315.887 (II)	Radial	Cu	63
Ti	334.941 (II)	Axial	Zn	66
Mn	257.610 (II)	Axial	Ga	71
Fe	259.940 (II)	Radial	As	75
			Rb	85
Minor elements			Y	89
Li	670.784 (I)	Axial	Zr	90
Be	313.042 (II)	Axial	Nb	93
Sc	361.384 (II)	Axial	Mo	95
V	292.402 (II)	Axial	Cd	111
Cr	267.716 (II)	Axial	Sn	120
Co	228.616 (II)	Axial	Sb	121
Ni	221.647 (II)	Axial	Cs	133
Cu	324.754 (I)	Axial	La	139
Zn	213.856 (I)	Axial	Ce	140
Sr	407.771 (II)	Axial	Pr	141
Y	360.073 (II)	Axial	Nd	146
Zr	343.823 (II)	Axial	Sm	147
Sn	189.989 (II)	Axial	Eu	151
Ba	455.403 (II)	Axial	Gd	157
Pb	220.353 (II)	Axial	Tb	159
			Dy	163
			Ho	165
			Er	167
			Tm	169
			Yb	173
			Lu	175
			Hf	178
			Ta	181
			Tl	205
			Pb	208
			Bi	209
			Th	232
			U	238

I: Originated from the neutral atom
II: Originated from the singly ionized state.

of Cd, Sn, Sb, Pb, and Bi concentrations in JSd-1 were 7–28% because of their low concentrations. The RSDs of Li and Be concentrations obtained using ICP-MS for all reference materials were 4–10% and 20–45%, respectively. The values were much larger than those of the other elements determined by ICP-MS and those determined by ICP-AES (3–4% for Li and 4–14% for Be). The ICP-MS operating in He collision mode effectively reduces polyatomic interfering ions and improves the accuracy for the analysis of minor elements. However, the sensitivities of Li and Be were strongly reduced in He collision mode. The Li and Be concentrations of JB-3 used for quality control were respectively 7.21 mg/kg and 0.81 mg/kg, which were much lower than those of stream sediments (JSd-1, -2, -3 and -4). The recovery rates of Li and Be in JB-3 determined using ICP-MS were systematically 10% and 20% lower than those measured using ICP-AES and the reference values, respectively. Thus, Li and Be concentrations measured by ICP-AES are preferable for geochemical mapping.

Table 4a Comparison of the analytical data of geochemical reference materials of stream sediments measured by ICP-AES.

Element	Unit	JSd-1 (*n=4*)	JSd-2 (*n=4*)	JSd-3 (*n=4*)	JSd-4 (*n=4*)	Reference			
		mean ± S.D.	mean ± S.D.	mean ± S.D.	mean ± S.D.	JSd-1[a]	JSd-2[a]	JSd-3[a]	JSd-4[b]
Na_2O	wt%	2.68 ± 0.01	2.41 ± 0.02	0.414 ± 0.006	2.23 ± 0.02	2.727	2.438	0.411	2.28
MgO	wt%	1.81 ± 0.01	2.76 ± 0.02	1.16 ± 0.01	4.01 ± 0.03	1.813	2.731	1.17	4.04
Al_2O_3	wt%	14.14 ± 0.37	11.70 ± 0.30	9.48 ± 0.29	12.54 ± 0.62	14.65	12.31	9.908	13.22
P_2O_5	wt%	0.123 ± 0.002	0.111 ± 0.001	0.081 ± <0.001	0.470 ± 0.002	0.122	0.105	0.0817	0.45
K_2O	wt%	2.15 ± 0.02	1.12 ± 0.01	1.97 ± 0.02	1.38 ± 0.02	2.183	1.145	1.971	1.40
CaO	wt%	3.05 ± 0.04	3.68 ± 0.03	0.568 ± 0.003	5.54 ± 0.07	3.034	3.658	0.56	5.57
TiO_2	wt%	0.649 ± 0.011	0.590 ± 0.005	0.408 ± 0.006	0.654 ± 0.012	0.643	0.614	0.403	0.64
MnO	wt%	0.094 ± 0.001	0.122 ± 0.001	0.150 ± 0.001	0.112 ± 0.001	0.0924	0.120	0.148	0.107
T-Fe_2O_3	wt%	5.02 ± 0.04	11.54 ± 0.10	4.38 ± 0.03	8.15 ± 0.07	5.059	11.65	4.368	8.06
H_2O^-	wt%	0.916 ± 0.002	0.606 ± 0.001	1.06 ± <0.01	5.04 ± <0.01	0.836	0.451	0.964	5.93
Li	mg/kg	22.8 ± 0.8	20.4 ± 0.6	152 ± 6	31.0 ± 1.0	22.8	19.2	151	32
Be	mg/kg	1.26 ± 0.09	0.91 ± 0.12	10.2 ± 0.4	1.12 ± 0.14	1.4	1.04	9.08	-
Sc	mg/kg	10.7 ± 0.2	17.8 ± 0.2	11.0 ± 0.4	16.2 ± 0.3	10.9	17.5	10.5	17
V	mg/kg	79.6 ± 0.8	128 ± 4	76.8 ± 2.1	150 ± 2	76	125	70.4	152
Cr	mg/kg	21.5 ± 0.5	95.5 ± 1.6	39.2 ± 0.8	1230 ± 29	21.5	108	35.3	1215
Ni	mg/kg	7.95 ± 0.34	97.4 ± 1.7	21.9 ± 0.8	113 ± 1	7.04	92.8	19.6	114
Cu	mg/kg	22.1 ± 1.1	1170 ± 25	452 ± 10	504 ± 8	22	1117	426	486
Zn	mg/kg	104 ± 2	2105 ± 35	148 ± 3	1506 ± 22	96.5	2056	136	1485
Sr	mg/kg	337 ± 7	208 ± 2	59.0 ± 0.9	215 ± 6	340	202	58.7	220
Y	mg/kg	14.5 ± 0.5	16.4 ± 0.3	11.8 ± 0.5	19.4 ± 0.5	14.8	17.4	14.9	21
Zr	mg/kg	20.9 ± 0.3	32.8 ± 0.5	49.1 ± 1.0	81.2 ± 1.6	132	111	124	90
Sn	mg/kg	n.d.	31.3 ± 3.7	102 ± 3	40.6 ± 1.3	2.77	32.5	195	-
Ba	mg/kg	549 ± 7	1287 ± 12	486 ± 8	874 ± 17	520	1199	462	888
Pb	mg/kg	n.d.	164 ± 3	87.0 ± 2.2	260 ± 4	12.9	146	82.1	240

[a]Imai *et al* . (1996), [b]Certificate of GSJ CRM

4. 2 Evaluation of arsenic analysis in geochemical reference materials

The addition of a strong oxidizing agent ($KMnO_4$) and the short decomposition time (20 min) prevents arsenic in sediments from volatilizing during digestion and the evaporation process (Terashima, 1976). Permanganic acid totally oxidizes As(III) to As(V) in a mixed acid solution, even for soil and sediments containing a large amount of reducing agent, such as organic matter. However, adequately recovering As during the digestion without using $KMnO_4$ and determining As concentrations with the other minor elements in the same experimental run would increase efficiency. Therefore, we compared the arsenic analyses obtained using the different methods.

Table 5 shows the As concentrations in eight Japanese geochemical reference materials sediment series (JLk-1, JSd-1–4, JMs-1, -2, and JSO-1) determined using different methods. When samples was decomposed using a mixed acid solution with $KMnO_4$ 120°C for 2 h and at 125–145°C for 3 h, arsenic concentrations decreased by 8% and by 15–20% relative to the original data, respectively. The decomposition without using a $KMnO_4$ provided the 10–40% lower of As concentrations than the original data irrespective of the decomposition times. These results are consistent with the observations that the As concentrations determined by digesting samples in a HF-HNO_3-H_2SO_4 solution without $KMnO_4$, which were subcontracted to Mitsubishi Materials Techno Co., were also much lower than the reference values (Table 5). Finally, the concentrations and repeatability errors (n = 4) of arsenic in JSd-1–4, which were determined using the method of Terashima (1976), are shown in Table 4b. The values were comparable to the reference values.

4. 3 Evaluation of the analysis of mercury in geochemical reference materials

Table 6 summarizes the Hg measurement of 14 geochemical reference materials. The Hg determination by a mercury analyzer "MA-2000" had a larger margin of error. The RSDs of mercury measurement were 1–9% for most materials, but were 16% for JMs-2 and 24% for JMn-1, whose Hg concentrations are the lowest among samples. The estimated values of JLk-1, JSd-2, JSd-3, JMs-1, JMs-2, JSl-1, and JSl-2 were similar to the reference data, although those of JSd-1 and JCFA-1 were rather

Table 4b Comparison of the analytical data of geochemical reference materials of stream sediments measured by ICP-MS.

Element	Unit	JSd-1 (*n=4*)	JSd-2 (*n=4*)	JSd-3 (*n=4*)	JSd-4 (*n=4*)	Reference			
		mean ± S.D.	mean ± S.D.	mean ± S.D.	mean ± S.D.	JSd-1[a]	JSd-2[a]	JSd-3[a]	JSd-4[b]
Li	mg/kg	22.8 ± 2.2	20.2 ± 1.9	149 ± 6	29.7 ± 1.9	22.8	19.2	151	32
Be	mg/kg	1.29 ± 0.33	1.17 ± 0.39	10.5 ± 2.0	0.90 ± 0.41	1.4	1.04	9.08	-
Sc	mg/kg	10.6 ± 0.1	17.4 ± 0.1	10.1 ± 0.5	16.1 ± 0.3	10.9	17.5	10.5	17
Cr	mg/kg	22.5 ± 1.6	95.0 ± 2.5	38.0 ± 0.8	1277 ± 22	21.5	108	35.3	1215
Co	mg/kg	11.1 ± 0.3	49.4 ± 0.9	12.5 ± 0.2	20.1 ± 0.4	11.2	48.4	12.7	21
Ni	mg/kg	7.61 ± 0.27	94.0 ± 2.3	19.2 ± 0.7	109 ± 3	7.04	92.8	19.6	114
Cu	mg/kg	23.9 ± 0.7	1139 ± 29*	435 ± 15	494 ± 12	22	1117	426	486
Zn	mg/kg	103 ± 3	2101 ± 51	143 ± 5	1495 ± 39	96.5	2056	136	1485
Ga	mg/kg	16.2 ± 0.4	13.4 ± 0.2	13.2 ± 0.4	14.5 ± 0.2	17.2	15.3	13.5	-
As	mg/kg	2.23 ± 0.06	40.5 ± 0.7	244 ± 28	55.9 ± 2.5	2.42	38.6	252	-
Rb	mg/kg	67.2 ± 1.9	26.1 ± 0.3	285 ± 6	50.7 ± 0.5	67.4	26.9	285	57
Y	mg/kg	14.3 ± 0.7	15.9 ± 0.3	11.1 ± 0.5	19.0 ± 0.5	14.8	17.4	14.9	21
Zr	mg/kg	19.9 ± 0.3	30.0 ± 0.7	46.6 ± 1.2	79.3 ± 0.6	132	111	124	90
Nb	mg/kg	10.7 ± 0.3	3.77 ± 0.11	6.87 ± 0.25	6.50 ± 0.17	11.1	4.56	7.8	-
Mo	mg/kg	0.474 ± 0.014	15.9 ± 0.6	1.62 ± 0.06	5.03 ± 0.19	0.45[c]	14.5[c]	1.73[c]	-
Cd	mg/kg	0.150 ± 0.011	3.16 ± 0.15	1.00 ± 0.05	6.68 ± 0.28	0.146	3.17	1.045	-
Sn	mg/kg	1.88 ± 0.17	30.1 ± 3.5	93.3 ± 1.8	40.1 ± 1.6	2.77	32.5	195	-
Sb	mg/kg	0.37 ± 0.10	11.9 ± 0.9	1.89 ± 0.06	7.52 ± 0.34	0.37	12.5	2.78	-
Cs	mg/kg	2.01 ± 0.12	1.02 ± 0.06	30.6 ± 1.1	3.78 ± 0.11	1.89	1.07	30.6	-
La	mg/kg	15.9 ± 0.8	10.1 ± 0.2	18.5 ± 0.7	16.1 ± 0.5	18.1	11.3	19.8	16
Ce	mg/kg	31.3 ± 1.4	20.5 ± 0.7	40.3 ± 1.6	31.9 ± 1.8	34.4	23.4	42	-
Pr	mg/kg	4.03 ± 0.18	2.76 ± 0.07	4.26 ± 0.18	3.84 ± 0.13	4.05	2.4	3.09	-
Nd	mg/kg	16.3 ± 0.7	11.7 ± 0.1	15.9 ± 0.6	15.3 ± 0.3	17.6	13.2	15.7	-
Sm	mg/kg	3.50 ± 0.09	2.78 ± 0.13	3.07 ± 0.12	3.32 ± 0.10	3.48	2.68	3.26	-
Eu	mg/kg	0.925 ± 0.034	0.801 ± 0.021	0.646 ± 0.033	0.856 ± 0.024	0.925	0.81	0.686	-
Gd	mg/kg	3.03 ± 0.13	2.76 ± 0.05	2.58 ± 0.07	3.21 ± 0.05	2.71	2.67	2.63	-
Tb	mg/kg	0.432 ± 0.02	0.433 ± 0.009	0.36 ± 0.014	0.491 ± 0.005	0.431	0.44	0.368	-
Dy	mg/kg	2.43 ± 0.08	2.63 ± 0.06	2.04 ± 0.12	2.96 ± 0.03	2.23	2.86	2.22	-
Ho	mg/kg	0.484 ± 0.014	0.551 ± 0.017	0.393 ± 0.013	0.607 ± 0.015	0.318	0.678	0.443	-
Er	mg/kg	1.29 ± 0.08	1.53 ± 0.04	1.07 ± 0.05	1.72 ± 0.09	0.906	1.48	1.07	-
Tm	mg/kg	0.181 ± 0.007	0.214 ± 0.007	0.159 ± 0.008	0.250 ± 0.007	0.13	0.23	0.155	-
Yb	mg/kg	1.19 ± 0.07	1.35 ± 0.04	1.04 ± 0.05	1.64 ± 0.07	1.18	1.67	1.4	-
Lu	mg/kg	0.170 ± 0.008	0.183 ± 0.003	0.156 ± 0.009	0.249 ± 0.014	0.186	0.252	0.196	-
Hf	mg/kg	0.663 ± 0.024	0.809 ± 0.009	1.18 ± 0.03	2.00 ± 0.04	3.55	2.7	3.21	-
Ta	mg/kg	0.864 ± 0.044	0.380 ± 0.008	0.584 ± 0.021	0.826 ± 0.058	0.893	0.515	0.687	-
Tl	mg/kg	0.365 ± 0.014	0.472 ± 0.02	2.20 ± 0.06	0.904 ± 0.034	0.407	0.45	2.06	-
Pb	mg/kg	15.3 ± 1.3	161 ± 3	85.8 ± 2.6	255 ± 6	12.9	146	82.1	240
Bi	mg/kg	0.126 ± 0.013	1.11 ± 0.07	12.5 ± 0.34	5.65 ± 0.30	0.106[d]	1.36[d]	12.8[d]	-
Th	mg/kg	4.08 ± 0.10	2.23 ± 0.05	6.45 ± 0.22	5.07 ± 0.17	4.44	2.33	7.79	-
U	mg/kg	0.846 ± 0.033	0.909 ± 0.017	1.23 ± 0.03	2.40 ± 0.02	1.0	1.1	1.66	-

* n=3

[a]Imai *et al* . (1996), [b]Certificate of GSJ CRM, [c]Terashima (1997), [d]Terashima *et al* . (2002b)

10% higher than the reference data. Nonetheless, it can be concluded that the simple and quick measurement by MA-2000 without any pre-treatment has satisfactory accuracy for Hg measurement. Just for reference, Hg concentrations in geochemical reference materials of JSd-4, JSO-1, JMn-1 (ferromanganese nodule), and JCu-1 (copper ore) and JZn-1 (zinc ore), whose Hg concentrations have not been determined, were also measured.

4. 4 Evaluation of the analysis of multi-elements in stream sediments collected from remote islands of the Seto Inland Sea

Nationwide geochemical mapping has emphasized on the straightforward and rapid decomposition methodology because multi-elements in a large number of samples had to be measured for a short period as long as possible (Imai *et al.*, 2004). Stream and marine sediments were digested using the mixed acid solution of HF, HNO_3, and

Table 5 Measured As concentrations in geochemical reference materials determined using different decomposition conditions.

Digestion	Decomposition temperature and time	Acid concentration in analytical solution	As (mg/kg)							
			JLk-1	JSd-1	JSd-2	JSd-3	JSd-4	JMs-1	JMs-2	JSO-1
with $KMnO_4$	at 120°C for 20 min	0.6 mol/L HCl	29	2.2	41	273	57	18	35	7.7
with $KMnO_4$	at 120°C for 2 hr	0.6 mol/L HCl	29	2.2	41	250	57	17	34	7.4
with $KMnO_4$	at 125°C for 2 hr and 145°C for 1 hr	0.6 mol/L HCl	24	2.2	33	217	46	15	29	6.3
without $KMnO_4$	at 120°C for 20 min	0.6 mol/L HCl	19	2.0	30	254	50	18	42	7.6
without $KMnO_4$[a]	at 125°C for 2 hr and 145°C for 1 hr	0.35 mol/L HNO_3	15	1.6	23	205	43	15	30	6.1
Digestion using $HF\text{-}HNO_3\text{-}H_2SO_4$[b]			22	2.0	34	n.d.	46	17	34	n.d.
Reference			26.8[c]	2.42[c]	38.6[c]	252[c]	-	18[d]	35[d]	8.1[d]

[a]Decomposition method used for determining 51 elements using ICP-AES and ICP-MS, [b]Mitsubishi Materials Techno Co., [c]Imai *et al*. (1996), [d]Terashima *et al*. (2002a)

Table 6 Measured Hg concentrations in geochemical reference materials.

Sample	n	Mean ± S.D. (μg/kg)	Reference (μg/kg)
JLK-1	10	156 ± 6	142[a]
JSd-1	9	23 ± 2	15.5[a]
JSd-2	4	107 ± 1	106[a]
JSd-3	6	270 ± 15	254[a]
JSd-4	5	5019 ± 119	-
JMs-1	6	668 ± 32	600[b], 800[b]
JMs-2	8	9.4 ± 1.5	<10[b]
JSO-1	6	90 ± 5	-
JSl-1	6	63 ± 2	67[a]
JSl-2	8	35 ± 1	35.3[a]
JFCA-1	6	171 ± 5	130[b], 160[b]
JMn-1	8	7.7 ± 1.8	-
JCu-1	5	216 ± 12	-
JZn-1	8	17 ± 1	-

[a]Imai *et al* . (1996), [b]Geological Survey of Japan, AIST(2017) Geochemical chemical Reference samples Database

$HClO_4$ at 120˚C for more than 30 min, then evaporated to dryness under 200˚C (Imai, 1990). The rapid analysis is quantitative enough for determining 51 elements in stream and marine sediments and definitely effective for geochemical mapping (Imai *et al.*, 2010; Imai *et al.*, 2004).

In this study, the mixed acid solution with samples was further heated at 125˚C for 2 h and 145˚C for 1 h before the drying process to accelerate the decomposition of refractory minerals within a restricted time. Minakawa *et al.* (2001) reported that refractory rare earth minerals, including allanite and monazite, occur within pegmatite veins of the Ryoke and Hiroshima granite pegmatites in the Shikoku Island. Ohta *et al.* (2017) reported extreme enrichments of light REEs, Nb, Ta, and Th both in stream sediments of the northern Shikoku Island and marine sediments of the Seto Inland Sea. Therefore, we also wanted to critically evaluate the concentrations of elements included in refractory minerals.

Elemental analyses of stream sediments collected from the remote islands of the Seto Inland Sea have been conducted using the method in Imai (1990) (Ohta *et al.*, 2017). Fig. 3 shows the relationships between elemental concentrations determined in this study and the previous study for Al_2O_3, TiO_2, Fe_2O_3, Y, Zr, Nb, La, Yb, Ta, Hf, and Th. Data points plot linearly on the 1:1 line for Al_2O_3 and Fe_2O_3. The result is reasonable because Al_2O_3 is not abundantly included in refractory minerals, and over accumulated magnetite minerals were removed in advance. In contrast, almost all data determined in this study plotted above the 1:1 line for Nb, Zr, and Hf. For TiO_2, La, Yb and Ta, some samples with high concentrations plotted on the upper side of the 1:1 line. It was not possible to determine the significance of Th concentration changes with different decomposition methods because the concentrations varied widely. In general, the treatment in this study improved the elemental concentrations in sediment samples containing a high proportion of refractory minerals. The concentrations of Zr and Hf greatly increased by 30% on average, nonetheless their concentrations in JSd-1–3 were much lower than the reference values due to incomplete decomposition using the $HF\text{-}HNO_3\text{-}HCO_4$ solution (Table 4). The concentration of TiO_2 increased 10% on an average; those of light REEs and Nb increased 15%; and those of heavy REEs and Ta increased 5–10%. Recovery rates for heavy REEs improved less than those for light REEs. This indicates that the contribution of refractory minerals to total elemental concentrations for heavy REEs is not as high as those for light REEs in the sediment samples measured in this study.

As discussed previously, the elemental concentrations of Li, Be, Sc, Cr, Co, Ni, Cu, Zn, Zr, Y, Sn, and Pb were measured by ICP-AES and ICP-MS to crosscheck their concentrations. Fig. 4 indicates the relationship between elemental concentrations in stream sediment samples

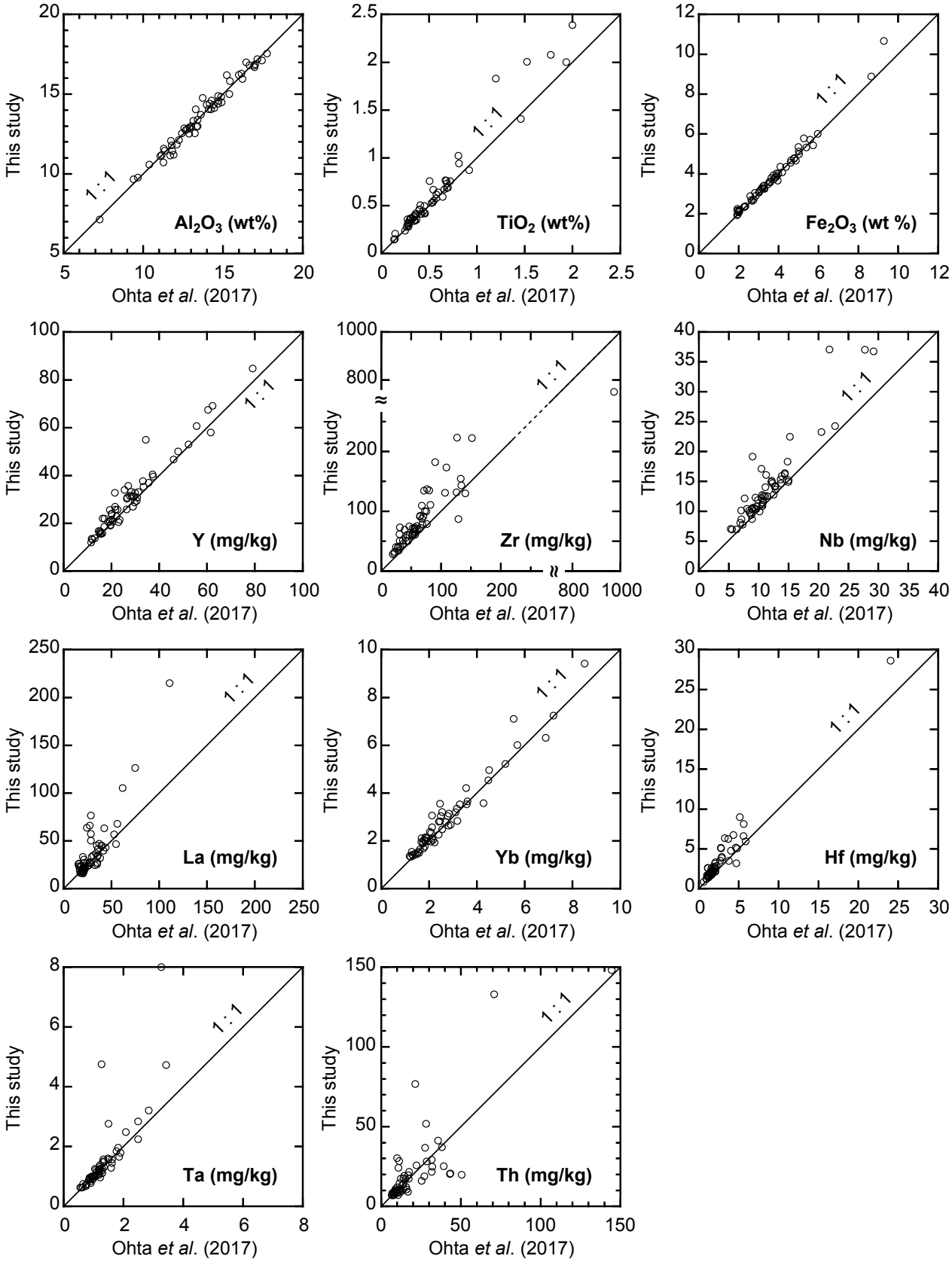

Fig. 3 Relationship between 11 elemental concentrations in stream sediments decomposed at 125–145°C for 3 h (this study) and room temperature for 30 min (Ohta *et al.*, 2017) before evaporated to dryness at 190–200°C.

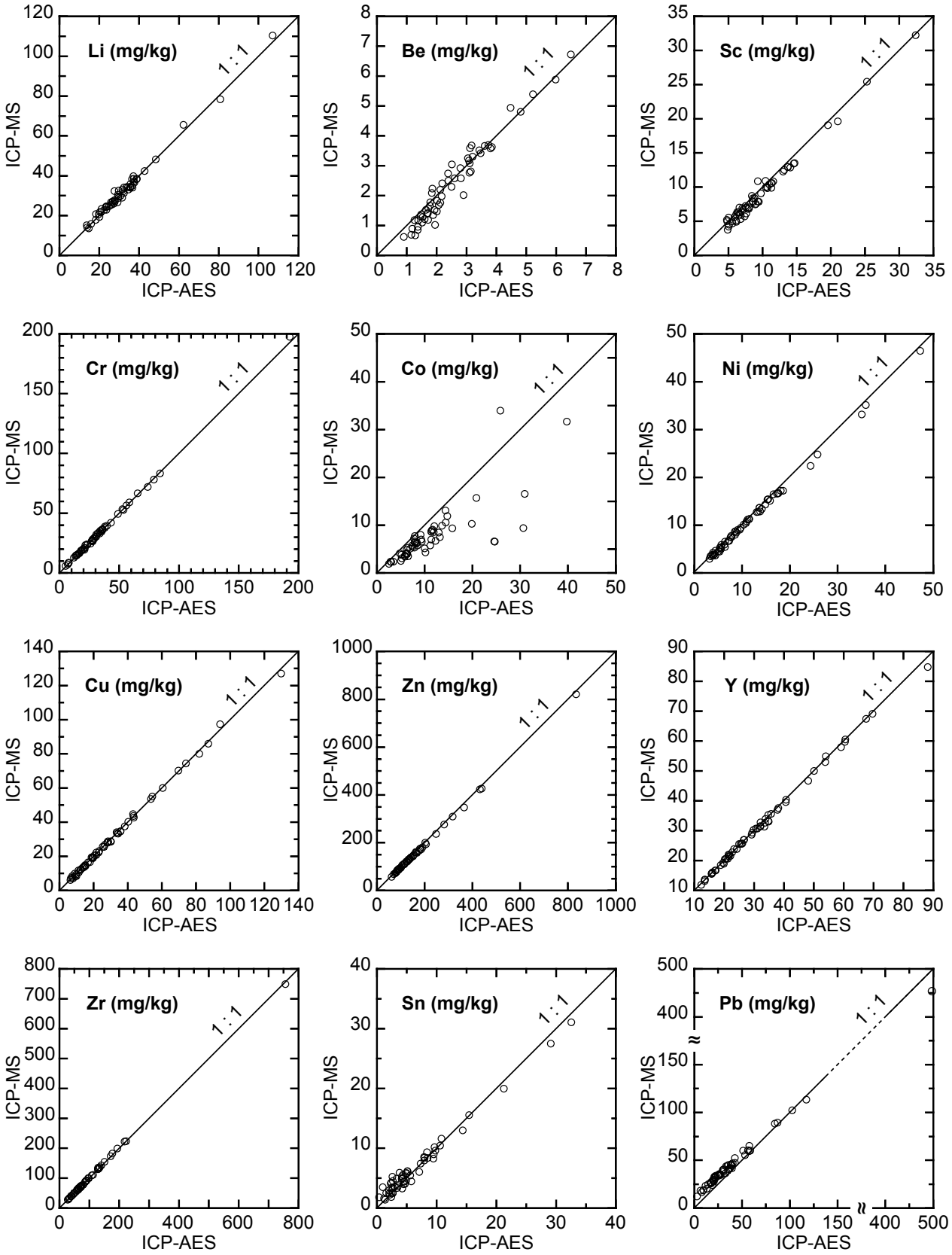

Fig. 4 Relationship between 12 elemental concentrations in stream sediment samples determined by ICP-AES and ICP-MS.

determined by ICP-AES and ICP-MS. Most data points plot on the 1:1 line for Li, Sc, Cr, Ni, Cu, Zn, Y, Zr, and Sn. However, a poor linearity was found for Be and Co data. ICP-MS measurement sensitivity for Li and Be in He collision mode is low as discussed previously. Especially, the sensitivity of Be in stream sediment sample was about a tenth part of that of Li, which caused the systematically lower Be concentrations. In contrast, Co concentrations determined by ICP-AES were approximately 1.5–2.0 times higher than those by ICP-MS. Cobalt concentrations in geochemical reference materials determined by ICP-MS were comparable to the certified values (Table 4b). Although the Pb concentrations determined with ICP-AES were highly correlated with those with ICP-MS, the ICP-AES provided systematically lower concentrations of Pb than the ICP-MS for samples with low concentrations (< 50 mg/kg). From those results, the ICP-AES is unsuitable for measuring Co and Pb for geochemical mapping.

Fig. 5 shows the As analyses of stream sediment samples in the mixed acid solution with and without $KMnO_4$. It was concluded that the decomposition without using $KMnO_4$ provides the systematically lower As concentrations in geochemical reference materials than reference values (Table 5). Nevertheless, the As concentrations determined without using $KMnO_4$ at 125–145°C for 3h were comparable to those determined using $KMnO_4$. This similarity is likely because the stream sediments samples in this study were collected mainly from granitic rock area and composed of visibly fine sands with a slight amount of silty and clayey size fractions and organic substances. Therefore, the usual analysis using HF-HNO_3-$HClO_4$ can save our time and effort to obtain high enough As quantities for geochemical mapping.

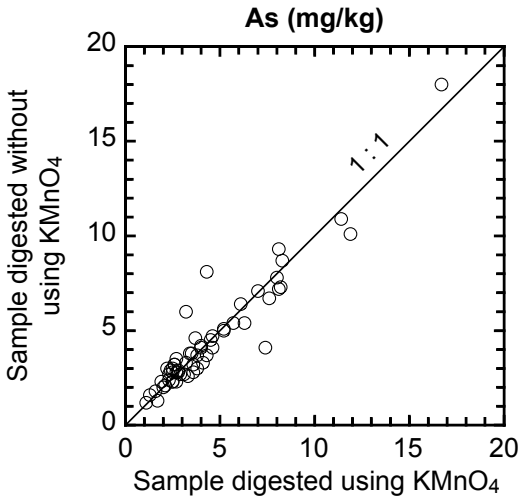

Fig. 5 Relationship between As concentrations in stream sediment samples determined using the mixed acid solutions with and without $KMnO_4$.

4. 5 Elemental concentrations in fine stream sediments collected from remote islands in the Seto Inland Sea

Table 7 summarizes the final analytical results of 53 elements in fine stream sediments (<180 μm) collected from remote islands of the Seto Inland Sea. The concentrations of the major elements, Li, Be, V, Sr, and Ba were determined by ICP-AES; the minor elements, except for Li, Be, V, Sr, Ba, and Hg, were measured by ICP-MS; and Hg was determined by AAS. Fig. 6 shows the geochemical maps for 12 elements on islands of the Seto Inland Sea and mainland (Honshu and Shikoku islands). Geochemical maps were prepared using GIS software. The methodology followed Ohta *et al.* (2004). The resultant geochemical maps in the remote islands were combined with the existing land geochemical maps of Ohta *et al.* (2017). Class selection of elemental concentrations used for geochemical mapping in the Chugoku and Shikoku regions (Ohta *et al.*, 2017) was also applied in this study.

As a whole, isolated islands were enriched in Na_2O, Al_2O_3, K_2O, Be, Rb, Nb, REEs, Cd, Sn, Ta, Hg, Tl, Pb, Th and U and depleted in MgO, CaO, TiO_2, Fe_2O_3, Sc, V, Cr, Co, Ni, Cu and Mo compared to the mainland. The western islands were rather enriched in P_2O_5, K_2O, MnO, Li, Be, Cu, Zn, As, Rb, Y, Zr, Nb, Mo, Cd, Sn, Sb, Cs, Sm, heavy REEs (Gd-Lu), Hf, Ta, Hg, Tl, Pb, Bi, Th, and U. Similar geochemical features were found in the northwest part of Shikoku Island and Hiroshima region, which is widely underlain with granitic rocks. In particular, sediments in Kurahashijima Island were highly enriched in Li, K_2O, Rb, Cs, and Tl. Their enrichments may have been caused by Cretaceous felsic volcanic intrusion (Fig. 1). Sediments in Yashirojima Island were abundant in light REEs (La-Sm) and Th and less abundant in heavy REEs. Sediments in Omishima Island and In-noshima Island showed the opposite trends to Yashirojima Island.

The eastern islands were abundant in MgO, CaO, TiO_2, V, Co, Sr, Ba, and Eu. Sediments in Shodoshima Island were enriched in MgO, TiO_2, V, Cr, MnO, Fe_2O_3, Ni, and Co, which are abundant in mafic volcanic rocks. The spatial distribution patterns of elements in Awajishima Island corresponded well to lithology. The high concentrations of Na_2O, Al_2O_3, CaO, TiO_2, MnO, Fe_2O_3, Sc, Ga, Nb, REEs, Ta, and Th in stream sediments were found in the northern part of Awajishima Island, which is primarily covered with Ryoke granitic rocks (Figs. 6(a), (b), and (d)). The enrichment in TiO_2, MnO, Fe_2O_3, and Sc may have been caused by the accumulation of ilmenite in the riverbed. Although excess magnetite minerals from samples were removed using a hand magnet, the magnetic property of ilmenite is much weaker than that of magnetite.

In contrast, the Cu, Zn, As, Mo, Cd, Sn, Sb, Hg, Pb, and Bi concentrations in stream sediments did not reflect the geology, and instead were influenced by mineral deposits and anthropogenic activity. Very high Cu, Zn, Cd, Sn, Sb, Hg, Pb, and Bi concentrations were found in Etajima Island, Osaki-kamijima Island, and Ikuchishima Island; these islands are associated with small scale Cu and W

Table 7 Analytical results of fine stream sediments (<180 μm) collected from remote islands in the Seto Inland Sea.

Element	Unit	Ys1	Ys2	Ys3	Kr1	Kr2	Kr3	Kr4	Et1	Et2	Et3
Na_2O	wt%	2.73	2.25	2.98	2.83	4.31	2.81	3.71	2.52	2.10	3.77
MgO	wt%	1.17	1.32	1.22	0.801	0.212	0.305	0.397	0.493	0.627	0.226
Al_2O_3	wt%	15.96	16.81	17.11	16.69	17.55	14.12	16.79	12.99	12.53	16.21
P_2O_5	wt%	0.170	0.178	0.146	0.119	0.073	0.166	0.207	0.110	0.136	0.115
K_2O	wt%	2.54	2.62	2.77	3.43	3.73	4.17	2.77	3.80	2.87	2.92
CaO	wt%	2.45	1.97	2.52	1.81	1.01	1.07	1.41	1.46	1.13	1.08
TiO_2	wt%	0.528	0.941	0.619	0.458	0.209	0.357	0.354	0.667	0.506	0.146
MnO	wt%	0.132	0.135	0.099	0.139	0.086	0.047	0.176	0.114	0.152	0.065
T-Fe_2O_3	wt%	4.06	4.75	4.53	4.00	2.11	1.96	3.77	2.87	3.20	2.04
Li	mg/kg	29.6	38.8	34.5	62.4	107	32.1	80.8	36.5	36.4	35.6
Be	mg/kg	2.1	2.2	2.1	3.8	6.0	3.2	4.8	3.4	3.2	5.2
Sc	mg/kg	8.72	9.86	9.97	10.9	6.35	4.51	8.41	10.9	6.82	4.26
V	mg/kg	41.3	45.1	35.4	41.4	12.8	16.9	22.1	31.9	32.3	11.1
Cr	mg/kg	32.3	38.9	35.4	18.8	8.27	14.9	15.6	27.4	34.8	8.49
Co	mg/kg	8.94	9.34	8.66	7.01	2.36	2.53	4.13	5.17	6.53	1.93
Ni	mg/kg	13.4	12.8	13.7	5.43	3.97	4.50	5.45	9.06	16.7	4.58
Cu	mg/kg	22.2	28.0	19.5	19.4	23.1	15.0	28.8	53.7	86.0	19.3
Zn	mg/kg	122	150	131	121	146	110	159	173	158	144
Ga	mg/kg	23.7	27.3	24.1	22.7	26.4	21.3	25.3	22.1	19.8	23.8
As	mg/kg	2.70	8.91	2.63	2.00	2.32	2.63	3.46	7.44	7.01	4.59
Rb	mg/kg	107	112	114	197	309	188	191	193	150	154
Sr	mg/kg	213	176	196	121	46.8	66.8	86.5	87.9	69.7	48.9
Y	mg/kg	22.0	35.7	25.7	53.0	67.4	32.8	60.6	69.1	33.2	84.8
Zr	mg/kg	28.3	50.6	73.6	222	135	137	173	749	111	130
Nb	mg/kg	11.9	14.9	14.7	15.1	22.5	12.3	18.3	37.1	17.1	15.9
Mo	mg/kg	0.533	0.718	0.521	0.769	0.825	0.737	1.05	17.5	1.06	1.08
Cd	mg/kg	0.228	0.205	0.220	0.214	0.413	0.265	0.248	0.713	0.339	0.512
Sn	mg/kg	4.82	5.85	3.61	9.60	15.6	5.26	11.6	20.0	9.71	5.93
Sb	mg/kg	0.598	0.431	0.241	0.675	2.47	0.718	1.11	3.39	1.52	0.611
Cs	mg/kg	3.39	4.04	3.02	10.4	14.4	5.29	11.4	7.29	6.42	5.99
Ba	mg/kg	563	465	549	264	200	406	258	320	340	244
La	mg/kg	76.7	126	50.5	34.6	23.2	63.8	41.5	105	67.8	45.4
Ce	mg/kg	159	261	97.4	63.5	61.3	136	84.5	225	146	87.2
Pr	mg/kg	17.6	28.5	11.7	8.21	6.93	16.2	10.3	26.3	16.8	12.4
Nd	mg/kg	65.4	103	43.9	31.9	27.7	61.0	38.9	99.3	62.6	48.4
Sm	mg/kg	11.6	17.8	8.17	7.37	8.02	13.4	8.92	21.8	13.2	11.9
Eu	mg/kg	1.16	1.24	1.13	0.862	0.395	0.536	0.749	0.660	0.571	0.613
Gd	mg/kg	8.58	13.2	6.45	6.98	7.61	9.70	8.32	15.3	9.74	11.4
Tb	mg/kg	1.00	1.57	0.862	1.17	1.38	1.27	1.36	2.13	1.20	1.78
Dy	mg/kg	4.85	7.76	4.69	7.66	9.32	6.29	8.81	12.0	6.14	11.2
Ho	mg/kg	0.774	1.22	0.854	1.65	2.02	1.10	1.83	2.38	1.10	2.35
Er	mg/kg	1.75	2.79	2.26	4.92	6.32	2.97	5.64	7.62	3.05	7.04
Tm	mg/kg	0.226	0.363	0.320	0.778	1.02	0.448	0.853	1.25	0.441	1.06
Yb	mg/kg	1.36	2.15	1.96	5.21	7.10	3.06	6.01	9.41	3.04	7.24
Lu	mg/kg	0.199	0.297	0.297	0.847	1.09	0.485	0.941	1.60	0.446	1.16
Hf	mg/kg	0.860	1.71	2.63	8.11	6.25	5.14	6.74	28.6	3.99	5.95
Ta	mg/kg	0.995	1.50	1.22	2.49	4.72	1.58	2.84	8.00	2.77	1.96
Hg	mg/kg	0.051	0.103	0.052	0.117	0.330	0.120	0.293	0.079	0.152	0.071
Tl	mg/kg	0.603	0.650	0.657	1.07	1.71	0.97	1.09	1.05	0.845	0.852
Pb	mg/kg	29.6	40.7	29.7	40.0	60.3	45.0	52.4	60.4	113	44.2
Bi	mg/kg	0.186	0.402	0.245	0.670	1.50	0.233	0.727	0.566	0.775	0.449
Th	mg/kg	28.4	51.8	19.5	20.3	36.7	76.8	29.3	148	41.3	28.2
U	mg/kg	3.05	5.86	3.36	11.9	11.8	8.37	9.68	26.7	7.91	8.01

Table 7 continued.

Element	Unit	Ok1	Ok2	Ok3	Ok4	Km1	Km2	Km3	Ik1	Ik2	In1
Na_2O	wt%	2.34	1.60	2.79	1.70	1.99	1.57	2.42	1.93	2.06	3.30
MgO	wt%	0.621	0.939	0.423	0.899	1.07	1.04	0.374	0.576	0.380	0.386
Al_2O_3	wt%	13.32	11.43	12.96	11.14	11.11	11.46	12.82	12.87	12.07	13.40
P_2O_5	wt%	0.140	0.177	0.149	0.218	0.151	0.148	0.103	0.338	0.216	0.146
K_2O	wt%	3.48	2.80	4.69	2.94	1.99	2.34	3.28	3.06	3.64	3.25
CaO	wt%	1.21	2.12	1.07	2.00	0.901	0.981	1.13	1.16	0.933	1.42
TiO_2	wt%	2.00	0.686	0.321	2.39	0.537	0.578	0.341	0.368	0.281	0.419
MnO	wt%	0.309	0.157	0.061	0.274	0.166	0.165	0.057	0.329	0.065	0.100
T-Fe_2O_3	wt%	4.32	3.86	2.14	5.32	3.57	3.81	2.32	3.25	2.11	2.17
Li	mg/kg	25.9	29.3	20.4	25.7	37.5	34.8	27.6	22.5	19.8	18.4
Be	mg/kg	2.6	1.9	3.0	2.0	1.7	1.8	2.5	3.1	3.8	3.1
Sc	mg/kg	9.07	7.87	3.78	10.0	6.15	7.47	4.94	7.26	6.30	6.04
V	mg/kg	42.5	41.4	18.4	44.6	45.4	48.6	19.9	28.0	25.1	21.4
Cr	mg/kg	30.4	35.8	23.9	83.3	59.1	52.9	36.1	42.1	33.1	33.1
Co	mg/kg	6.54	8.46	3.11	9.41	9.77	8.62	3.67	6.60	3.83	3.47
Ni	mg/kg	9.01	17.2	5.21	13.6	22.4	15.1	6.72	12.7	9.47	7.99
Cu	mg/kg	25.8	28.7	55.0	43.7	60.0	42.7	14.4	74.5	127	44.8
Zn	mg/kg	181	173	175	424	237	194	133	310	348	201
Ga	mg/kg	19.8	13.6	16.9	14.9	13.1	14.7	17.6	17.8	16.4	17.6
As	mg/kg	6.08	11.46	2.60	4.80	7.99	5.72	2.67	17.11	8.25	2.06
Rb	mg/kg	168	113	210	119	84.5	105	154	138	171	139
Sr	mg/kg	90.1	125	89.8	113	91.8	89.1	97.8	98.9	75.0	109
Y	mg/kg	46.8	20.7	25.7	31.5	16.8	21.6	23.9	32.7	33.0	23.9
Zr	mg/kg	224	59.9	135	92.7	56.0	73.2	69.8	69.5	78.9	101
Nb	mg/kg	36.7	11.5	12.2	37.0	9.77	12.6	14.0	12.6	12.2	14.3
Mo	mg/kg	1.29	0.871	0.451	1.20	0.876	1.03	0.427	1.19	0.966	0.839
Cd	mg/kg	0.301	0.448	0.251	0.957	0.468	0.343	0.507	0.818	7.99	0.319
Sn	mg/kg	13.0	7.98	5.35	10.2	7.43	4.45	4.94	9.00	8.55	4.52
Sb	mg/kg	1.00	0.846	0.542	1.12	1.10	0.945	0.583	0.772	0.662	0.494
Cs	mg/kg	5.02	5.33	4.26	4.91	6.60	7.61	7.79	5.53	5.06	4.36
Ba	mg/kg	452	530	689	514	387	391	543	485	476	499
La	mg/kg	39.6	19.2	16.3	34.9	20.8	23.6	30.6	27.8	20.1	19.6
Ce	mg/kg	122	39.8	35.3	58.4	39.3	45.1	59.1	56.5	39.4	35.6
Pr	mg/kg	9.88	4.74	4.00	7.67	4.83	5.43	6.84	6.58	5.05	4.62
Nd	mg/kg	37.3	18.2	15.3	26.9	18.2	20.8	24.8	24.2	19.8	17.4
Sm	mg/kg	8.27	3.80	3.55	5.22	3.54	4.21	4.83	5.08	4.58	3.66
Eu	mg/kg	0.671	0.750	0.540	0.868	0.663	0.690	0.693	0.741	0.565	0.634
Gd	mg/kg	7.58	3.57	3.27	4.87	3.10	3.81	4.21	4.77	4.68	3.46
Tb	mg/kg	1.14	0.528	0.547	0.766	0.468	0.570	0.624	0.749	0.787	0.564
Dy	mg/kg	6.97	3.27	3.59	4.72	2.69	3.39	3.62	4.77	5.08	3.49
Ho	mg/kg	1.46	0.651	0.777	0.970	0.541	0.689	0.738	0.977	1.03	0.746
Er	mg/kg	4.44	1.95	2.36	2.87	1.53	1.99	2.21	2.89	2.92	2.19
Tm	mg/kg	0.699	0.307	0.367	0.430	0.234	0.293	0.317	0.438	0.444	0.335
Yb	mg/kg	4.96	1.99	2.57	2.81	1.54	2.01	2.15	3.04	2.84	2.33
Lu	mg/kg	0.775	0.303	0.412	0.423	0.228	0.300	0.341	0.473	0.437	0.374
Hf	mg/kg	9.00	2.04	5.08	3.17	1.69	2.25	2.51	2.55	3.50	3.86
Ta	mg/kg	3.21	1.23	1.26	1.79	0.959	1.16	1.25	1.24	1.38	1.32
Hg	mg/kg	0.064	0.037	0.095	0.072	0.144	0.077	0.050	0.115	0.084	0.066
Tl	mg/kg	1.04	0.752	1.10	0.720	0.536	0.597	0.898	0.908	1.22	0.819
Pb	mg/kg	89.4	36.4	47.2	60.1	55.4	41.6	34.7	47.0	41.8	35.6
Bi	mg/kg	0.618	0.354	0.433	0.647	0.496	0.509	0.394	1.09	2.50	0.560
Th	mg/kg	24.8	8.59	19.8	14.4	8.36	9.20	12.0	13.1	10.9	12.2
U	mg/kg	6.79	2.28	4.24	5.19	2.25	3.05	2.87	3.37	3.64	3.48

Table 7 continued.

Element	Unit	Mk1	Os1	Os2	Ha1	Om1	Om2	Om3	Sd1	Sd2	Sd3
Na_2O	wt%	3.32	2.80	3.98	3.79	4.34	2.76	2.49	2.91	3.79	3.08
MgO	wt%	0.685	1.13	0.508	0.379	0.220	0.431	1.35	2.07	0.673	1.78
Al_2O_3	wt%	14.76	17.20	16.87	14.49	15.01	12.84	12.12	13.71	14.41	14.06
P_2O_5	wt%	0.423	0.298	0.088	0.105	0.045	0.068	0.289	0.177	0.169	0.235
K_2O	wt%	3.04	2.39	3.41	2.94	3.66	3.73	2.80	1.98	2.37	2.25
CaO	wt%	1.83	2.51	2.14	1.87	0.823	0.893	2.87	3.52	2.22	2.93
TiO_2	wt%	0.295	0.670	0.346	0.381	0.153	0.239	0.345	1.02	0.312	0.756
MnO	wt%	0.074	0.189	0.147	0.119	0.066	0.049	0.098	0.182	0.096	0.118
T-Fe_2O_3	wt%	3.38	5.99	3.21	3.27	1.91	2.33	3.70	5.75	3.01	4.72
Li	mg/kg	37.1	42.8	32.5	16.0	26.7	27.7	29.4	26.8	23.6	23.5
Be	mg/kg	3.6	2.9	3.1	2.8	4.5	2.8	2.5	2.2	3.1	2.4
Sc	mg/kg	6.34	13.5	5.74	10.6	5.56	5.23	7.02	12.9	5.33	10.8
V	mg/kg	23.8	37.2	20.8	12.3	20.6	28.3	37.8	80.7	23.8	60.7
Cr	mg/kg	33.7	15.1	8.67	12.8	7.15	14.8	56.5	78.3	21.1	66.7
Co	mg/kg	4.84	11.9	4.01	3.42	2.35	4.11	7.25	15.7	5.30	10.6
Ni	mg/kg	10.8	5.94	3.65	4.97	3.55	7.50	35.1	24.8	6.73	17.2
Cu	mg/kg	97.4	33.5	11.9	20.8	7.3	14.0	70.2	25.6	19.4	40.2
Zn	mg/kg	427	276	122	161	100	86.6	821	137	139	138
Ga	mg/kg	18.5	23.1	23.6	20.3	22.3	16.9	16.5	19.4	21.8	18.5
As	mg/kg	4.35	3.69	2.65	2.55	2.49	5.25	5.34	3.91	2.27	2.57
Rb	mg/kg	154	125	140	109	218	187	137	93.5	102	97.8
Sr	mg/kg	132	165	231	142	58.6	71.5	140	223	180	216
Y	mg/kg	30.3	40.4	29.5	35.3	58.0	39.6	37.7	22.8	25.6	20.8
Zr	mg/kg	131	50.2	34.7	91.5	143	132	87.2	61.1	59.5	72.0
Nb	mg/kg	10.4	16.2	13.6	10.5	15.3	9.81	19.2	12.7	10.4	11.9
Mo	mg/kg	2.18	0.415	0.396	0.567	0.530	0.422	1.72	0.993	0.462	0.791
Cd	mg/kg	0.410	0.547	0.238	0.319	0.330	0.346	1.38	0.253	0.279	0.284
Sn	mg/kg	8.27	5.08	3.50	4.01	6.16	5.58	8.38	5.86	4.62	4.15
Sb	mg/kg	1.18	0.472	0.282	0.381	0.480	0.421	2.124	0.404	0.372	0.787
Cs	mg/kg	7.61	4.39	3.68	2.80	4.68	5.58	4.80	4.64	3.97	5.26
Ba	mg/kg	349	361	518	728	216	345	337	423	444	447
La	mg/kg	22.6	33.4	45.1	26.7	17.8	22.5	18.7	57.3	66.1	26.7
Ce	mg/kg	52.7	63.3	84.7	58.0	35.9	34.2	35.9	118	132	54.3
Pr	mg/kg	5.11	8.61	10.2	6.74	5.11	5.66	4.75	13.5	15.5	6.25
Nd	mg/kg	18.8	33.8	37.1	26.4	20.4	22.2	18.4	49.3	57.6	23.5
Sm	mg/kg	4.12	7.66	7.06	6.09	5.85	5.09	4.42	7.47	11.68	4.58
Eu	mg/kg	0.702	1.10	0.966	1.00	0.476	0.553	0.647	0.874	0.926	0.877
Gd	mg/kg	3.96	7.19	5.79	5.91	6.30	4.86	4.86	5.53	8.53	3.94
Tb	mg/kg	0.633	1.05	0.820	0.922	1.16	0.750	0.871	0.685	1.03	0.565
Dy	mg/kg	4.12	6.23	4.71	5.74	8.08	4.75	5.88	3.91	4.81	3.41
Ho	mg/kg	0.902	1.28	0.927	1.19	1.75	1.05	1.26	0.751	0.827	0.681
Er	mg/kg	2.78	3.59	2.57	3.34	5.54	3.20	3.83	2.15	2.15	1.93
Tm	mg/kg	0.448	0.529	0.381	0.494	0.894	0.508	0.616	0.310	0.301	0.295
Yb	mg/kg	3.19	3.53	2.48	3.35	6.31	3.53	4.22	2.10	1.95	2.05
Lu	mg/kg	0.505	0.523	0.354	0.498	0.995	0.585	0.619	0.309	0.295	0.299
Hf	mg/kg	4.78	1.93	1.42	3.52	6.62	5.17	3.20	1.95	2.26	2.30
Ta	mg/kg	1.45	1.84	1.57	0.956	2.25	1.49	1.27	1.02	1.18	1.03
Hg	mg/kg	0.214	0.092	0.034	0.047	0.032	0.033	0.103	0.060	0.060	0.082
Tl	mg/kg	0.894	0.737	0.750	0.596	1.18	1.05	0.857	0.538	0.579	0.560
Pb	mg/kg	65.1	33.8	32.9	33.6	43.7	34.9	88.2	29.3	31.9	26.1
Bi	mg/kg	0.831	0.630	0.466	0.305	0.775	0.630	1.02	0.439	0.291	0.360
Th	mg/kg	17.7	14.2	21.6	25.2	16.0	37.1	18.8	30.3	24.1	10.8
U	mg/kg	6.20	3.70	2.91	3.38	6.09	6.33	4.96	2.50	3.42	2.57

Table 7 continued.

Element	Unit	Sd4	Sd5	Sd6	Sd7	Sd8	Aw1	Aw2	Aw3	Aw4	Aw5
Na_2O	wt%	3.46	4.65	3.77	3.09	2.72	2.88	3.34	3.49	1.84	2.19
MgO	wt%	0.992	1.22	0.835	1.77	5.93	1.42	0.877	0.727	0.562	0.488
Al_2O_3	wt%	14.04	16.29	16.19	16.99	12.99	15.83	14.61	14.34	12.54	11.19
P_2O_5	wt%	0.136	0.101	0.090	0.124	0.102	0.231	0.103	0.086	0.104	0.118
K_2O	wt%	2.64	2.26	2.62	2.35	1.20	2.41	2.68	2.54	2.69	2.73
CaO	wt%	2.34	2.28	2.11	3.16	4.18	1.48	2.27	1.74	0.689	1.02
TiO_2	wt%	0.765	0.318	0.281	0.554	1.83	0.732	0.422	0.415	0.497	0.763
MnO	wt%	0.224	0.095	0.157	0.177	0.280	0.119	0.102	0.090	0.066	0.098
T-Fe_2O_3	wt%	3.91	3.09	3.34	5.67	10.66	5.29	3.81	3.25	3.55	2.66
Li	mg/kg	20.9	35.6	35.7	33.8	29.5	37.7	23.6	23.7	31.7	23.5
Be	mg/kg	2.4	3.7	3.5	3.1	2.1	2.0	1.8	1.9	1.7	1.4
Sc	mg/kg	7.92	6.86	7.57	13.5	25.4	12.5	7.96	6.76	8.39	6.92
V	mg/kg	39.0	43.6	34.6	63.8	190	53.4	25.7	32.8	42.2	36.0
Cr	mg/kg	30.2	53.5	36.4	49.4	198	39.5	20.2	27.1	23.3	27.5
Co	mg/kg	6.73	34.0	7.71	13.1	31.7	9.92	6.37	6.35	5.78	5.76
Ni	mg/kg	11.3	16.5	16.7	16.6	46.4	12.9	7.76	10.5	8.73	7.49
Cu	mg/kg	26.8	28.2	20.8	28.8	34.2	34.5	16.6	13.8	22.3	11.8
Zn	mg/kg	130	121	144	132	130	167	95.6	89.8	89.1	68.6
Ga	mg/kg	20.5	34.1	22.8	23.7	18.9	21.5	18.2	17.2	15.9	12.5
As	mg/kg	3.91	3.24	4.05	4.17	2.44	8.60	2.77	2.11	7.74	3.32
Rb	mg/kg	98.9	105	130	129	63.8	108	97.5	97.2	115	103
Sr	mg/kg	184	134	109	214	200	139	195	188	96.0	126
Y	mg/kg	26.9	55.0	34.0	30.8	27.0	31.4	19.3	16.1	20.7	15.8
Zr	mg/kg	74.7	182	75.8	110	155	63.3	41.1	40.9	87.8	60.8
Nb	mg/kg	16.4	11.2	14.2	14.1	16.1	14.7	10.9	9.38	10.7	12.6
Mo	mg/kg	1.19	0.459	2.93	0.824	0.523	0.975	0.405	0.395	0.713	1.10
Cd	mg/kg	0.142	0.348	0.619	0.295	0.191	0.168	0.102	0.099	0.177	0.156
Sn	mg/kg	4.02	4.25	5.48	4.89	3.29	4.50	9.37	10.5	4.50	2.96
Sb	mg/kg	0.651	0.650	0.517	0.483	0.264	0.818	0.329	0.481	0.916	0.510
Cs	mg/kg	3.79	4.69	5.78	6.58	3.65	5.51	2.82	2.88	6.81	3.41
Ba	mg/kg	548	359	358	472	211	462	583	542	509	638
La	mg/kg	63.2	215	23.6	47.1	33.4	45.1	25.5	26.8	24.5	18.3
Ce	mg/kg	129	466	55.4	106	75.9	88.8	47.0	51.2	49.5	34.4
Pr	mg/kg	14.4	53.5	6.91	11.4	8.96	10.5	5.61	5.64	5.79	4.01
Nd	mg/kg	52.3	198	27.3	41.3	34.8	38.3	20.4	20.0	21.1	14.6
Sm	mg/kg	9.78	43.7	7.05	8.23	7.80	7.19	3.85	3.74	4.10	2.83
Eu	mg/kg	0.978	0.807	0.653	0.899	0.825	1.18	0.901	0.768	0.714	0.619
Gd	mg/kg	7.60	30.7	6.13	6.92	6.05	6.16	3.45	3.16	3.55	2.57
Tb	mg/kg	0.950	3.42	0.935	0.978	0.789	0.899	0.496	0.450	0.544	0.393
Dy	mg/kg	4.86	14.6	5.53	5.32	4.46	5.36	3.09	2.60	3.40	2.45
Ho	mg/kg	0.886	2.08	1.10	1.01	0.887	1.03	0.624	0.519	0.707	0.522
Er	mg/kg	2.46	4.49	3.07	2.85	2.67	2.86	1.79	1.45	2.04	1.50
Tm	mg/kg	0.351	0.566	0.473	0.410	0.453	0.419	0.267	0.217	0.311	0.227
Yb	mg/kg	2.38	3.55	3.21	2.82	3.58	2.79	1.77	1.44	2.10	1.55
Lu	mg/kg	0.377	0.522	0.493	0.424	0.566	0.414	0.268	0.216	0.310	0.242
Hf	mg/kg	2.68	6.36	2.78	3.33	5.07	2.07	1.53	1.52	2.58	1.94
Ta	mg/kg	1.31	1.19	1.60	1.57	1.10	1.26	0.988	0.908	0.910	0.994
Hg	mg/kg	0.060	0.028	0.061	0.045	0.032	0.119	0.026	0.032	0.057	0.061
Tl	mg/kg	0.535	0.563	0.783	0.714	0.347	0.633	0.534	0.519	0.672	0.588
Pb	mg/kg	28.6	31.9	34.6	32.8	45.9	34.8	38.0	35.7	33.9	59.5
Bi	mg/kg	0.305	0.174	0.429	0.352	0.180	0.383	0.117	0.146	0.279	0.174
Th	mg/kg	19.1	133	17.4	25.6	20.6	17.1	8.73	9.64	9.61	7.41
U	mg/kg	2.99	8.27	3.27	4.59	3.61	2.56	1.66	1.80	2.39	1.75

Table 7 continued.

Element	Unit	Aw6	Aw7	Aw8	Aw9	Aw10	Aw11	Aw12	Aw13	Aw14	Aw15
Na_2O	wt%	2.10	1.97	1.67	1.23	1.98	2.06	2.12	2.68	2.12	1.98
MgO	wt%	0.537	0.507	0.595	0.523	0.509	0.688	0.725	0.765	0.673	0.556
Al_2O_3	wt%	10.59	9.76	11.78	7.13	9.66	11.59	12.92	11.84	11.20	10.72
P_2O_5	wt%	0.127	0.098	0.171	0.128	0.094	0.110	0.067	0.074	0.098	0.127
K_2O	wt%	2.47	2.44	2.38	2.02	2.35	2.58	2.51	2.39	2.31	2.64
CaO	wt%	0.695	0.581	0.493	0.590	0.475	0.524	0.465	1.88	1.10	0.781
TiO_2	wt%	0.353	0.367	0.402	0.757	0.367	0.370	0.459	0.420	0.443	0.391
MnO	wt%	0.049	0.039	0.080	0.062	0.032	0.061	0.039	0.072	0.074	0.065
T-Fe_2O_3	wt%	2.35	2.07	3.04	2.21	2.16	2.88	3.47	3.65	2.69	2.64
Li	mg/kg	29.7	30.8	37.5	27.7	31.6	36.8	38.8	26.4	27.9	32.4
Be	mg/kg	1.3	1.2	1.6	0.91	1.2	1.5	1.7	1.5	1.4	1.4
Sc	mg/kg	5.64	4.97	7.05	5.10	4.69	5.93	7.82	10.6	7.03	5.99
V	mg/kg	32.3	30.1	38.8	37.9	30.0	34.5	50.5	35.8	39.0	38.5
Cr	mg/kg	24.1	21.0	28.9	71.9	37.9	24.7	26.7	18.2	36.8	28.7
Co	mg/kg	4.15	4.06	8.03	4.32	4.00	5.78	5.33	5.50	6.15	5.12
Ni	mg/kg	8.69	8.44	15.4	33.2	15.4	11.2	11.3	6.58	14.3	10.1
Cu	mg/kg	14.6	13.7	33.4	80.1	37.6	34.8	16.5	10.7	13.1	18.8
Zn	mg/kg	86.4	72.3	125	57.1	88.1	109	79.8	84.8	75.7	106
Ga	mg/kg	11.6	11.4	14.7	8.7	10.5	12.9	15.5	15.0	13.0	12.7
As	mg/kg	4.38	3.65	8.33	3.64	4.11	6.41	12.1	2.90	3.10	4.71
Rb	mg/kg	96.1	93.3	108	74.9	90.2	104	109	91.4	88.2	104
Sr	mg/kg	122	111	90.3	84.9	107	106	108	166	122	120
Y	mg/kg	13.7	13.6	22.0	11.9	13.2	16.7	18.6	20.5	15.6	15.7
Zr	mg/kg	66.4	66.4	91.6	71.4	69.8	78.2	99.8	50.0	60.8	72.7
Nb	mg/kg	6.97	7.09	10.4	10.1	7.01	8.12	10.2	8.74	7.77	8.69
Mo	mg/kg	0.375	0.266	0.744	0.414	0.371	0.730	0.780	0.552	0.587	0.660
Cd	mg/kg	0.146	0.114	0.253	0.181	0.167	0.165	0.126	0.142	0.150	0.167
Sn	mg/kg	6.03	2.43	3.69	27.5	31.1	8.45	3.39	3.42	2.24	3.38
Sb	mg/kg	1.22	0.963	1.40	1.48	1.10	1.19	1.41	0.525	0.789	0.962
Cs	mg/kg	3.78	3.72	6.51	2.83	3.51	5.14	6.98	3.00	3.60	4.30
Ba	mg/kg	559	532	559	464	523	504	482	499	521	598
La	mg/kg	16.6	26.3	23.0	25.8	18.3	19.4	21.8	27.2	16.0	21.4
Ce	mg/kg	31.9	50.1	45.9	49.3	35.5	39.0	45.6	53.2	32.4	38.7
Pr	mg/kg	3.74	5.49	5.54	5.25	4.01	4.46	5.18	6.05	3.72	4.56
Nd	mg/kg	13.2	18.9	20.8	18.1	14.3	16.4	19.1	22.1	13.6	16.1
Sm	mg/kg	2.59	3.27	4.24	2.81	2.72	3.16	3.73	4.19	2.83	2.97
Eu	mg/kg	0.560	0.581	0.791	0.454	0.543	0.651	0.673	0.777	0.656	0.554
Gd	mg/kg	2.23	2.69	3.88	2.27	2.20	2.72	3.26	3.69	2.46	2.45
Tb	mg/kg	0.341	0.364	0.556	0.316	0.347	0.422	0.491	0.551	0.378	0.381
Dy	mg/kg	2.18	2.17	3.57	1.91	2.13	2.59	3.04	3.33	2.48	2.46
Ho	mg/kg	0.452	0.462	0.724	0.404	0.457	0.543	0.628	0.672	0.507	0.524
Er	mg/kg	1.38	1.34	2.20	1.23	1.36	1.67	1.91	1.97	1.57	1.57
Tm	mg/kg	0.202	0.203	0.312	0.189	0.205	0.251	0.279	0.294	0.227	0.235
Yb	mg/kg	1.45	1.42	2.12	1.33	1.38	1.65	1.90	1.93	1.50	1.70
Lu	mg/kg	0.217	0.216	0.309	0.210	0.220	0.259	0.295	0.290	0.223	0.251
Hf	mg/kg	1.96	1.94	2.63	2.17	2.01	2.22	2.87	1.74	1.84	2.14
Ta	mg/kg	0.636	0.634	0.877	0.756	0.631	0.731	0.927	0.777	0.679	0.729
Hg	mg/kg	0.096	0.080	0.078	0.356	0.078	0.071	0.049	0.042	0.061	0.085
Tl	mg/kg	0.562	0.565	0.647	0.466	0.546	0.604	0.621	0.533	0.510	0.605
Pb	mg/kg	40.6	39.1	27.8	453	102	45.2	25.9	18.6	20.1	44.9
Bi	mg/kg	0.173	0.141	0.453	0.311	0.145	0.290	0.484	0.143	0.163	0.169
Th	mg/kg	6.95	8.71	9.86	6.93	7.22	8.27	9.80	10.6	8.74	8.26
U	mg/kg	1.73	1.67	2.51	1.69	1.66	2.08	2.22	1.78	1.75	1.85

Table 7 continued.

Element	Unit	Aw16	Aw17	Aw18	Aw19	Aw20	Aw21	Aw22	Aw23
Na_2O	wt%	3.36	3.05	3.12	2.68	2.75	2.59	2.61	2.52
MgO	wt%	0.922	0.998	1.05	2.76	1.11	1.57	1.21	0.782
Al_2O_3	wt%	14.83	14.88	14.34	14.05	14.41	12.54	14.58	12.75
P_2O_5	wt%	0.094	0.155	0.089	0.189	0.099	0.086	0.068	0.056
K_2O	wt%	2.54	2.46	2.36	1.38	2.16	2.09	2.41	2.53
CaO	wt%	2.22	2.32	2.88	5.18	2.75	3.17	2.88	1.87
TiO_2	wt%	0.415	0.872	0.691	2.08	0.593	1.41	0.639	2.00
MnO	wt%	0.163	0.134	0.114	0.236	0.099	0.167	0.140	0.160
T-Fe_2O_3	wt%	4.00	4.98	4.33	8.89	4.63	5.41	5.10	4.67
Li	mg/kg	27.4	24.8	18.2	13.7	21.3	14.0	14.8	20.1
Be	mg/kg	1.9	1.8	1.7	1.3	1.5	1.5	2.0	1.6
Sc	mg/kg	10.4	12.3	12.9	32.2	13.0	19.1	19.6	9.91
V	mg/kg	30.2	38.2	38.5	85.0	46.4	66.2	57.0	46.1
Cr	mg/kg	14.1	18.9	16.3	27.7	19.5	26.7	16.6	19.5
Co	mg/kg	6.39	7.50	7.02	16.6	9.08	10.3	8.54	6.62
Ni	mg/kg	3.67	5.87	2.98	4.64	3.83	4.27	3.55	5.34
Cu	mg/kg	8.58	12.6	7.52	8.58	9.43	7.30	6.11	9.93
Zn	mg/kg	92.1	114	86.3	112	86.4	84.4	78.3	77.9
Ga	mg/kg	18.9	20.5	18.0	19.5	17.1	16.0	17.3	15.2
As	mg/kg	3.21	2.83	1.11	1.35	3.80	2.87	1.67	1.70
Rb	mg/kg	103	99.0	89.7	45.1	80.6	73.2	85.8	90.6
Sr	mg/kg	194	196	209	236	206	178	171	144
Y	mg/kg	25.8	30.8	28.7	50.0	21.4	31.5	37.0	19.0
Zr	mg/kg	51.7	45.8	29.9	40.3	32.2	61.8	38.7	69.4
Nb	mg/kg	10.4	14.9	12.8	23.3	10.0	15.2	10.9	24.3
Mo	mg/kg	0.459	0.605	0.306	0.202	0.369	0.341	0.574	0.352
Cd	mg/kg	0.157	0.178	0.086	0.134	0.093	0.132	0.115	0.082
Sn	mg/kg	2.58	2.54	1.80	1.40	1.63	1.87	2.52	2.53
Sb	mg/kg	0.394	0.379	0.178	0.113	0.234	0.238	0.164	0.301
Cs	mg/kg	3.39	3.47	2.30	1.25	2.36	1.99	2.10	2.77
Ba	mg/kg	539	547	521	371	518	494	558	554
La	mg/kg	32.2	56.7	33.5	46.6	24.6	43.0	27.1	37.1
Ce	mg/kg	54.2	108	62.7	96.2	47.8	87.0	60.3	69.8
Pr	mg/kg	6.91	11.8	7.29	11.4	5.54	9.33	7.14	7.56
Nd	mg/kg	25.4	41.3	26.6	44.3	20.6	33.7	28.4	26.5
Sm	mg/kg	4.92	7.11	5.08	9.13	4.04	6.09	6.31	4.61
Eu	mg/kg	0.960	1.07	0.989	1.36	0.926	0.934	0.919	0.850
Gd	mg/kg	4.33	6.10	4.67	8.70	3.71	5.33	6.02	3.69
Tb	mg/kg	0.646	0.859	0.715	1.30	0.550	0.804	0.921	0.514
Dy	mg/kg	3.99	5.17	4.64	8.25	3.43	5.00	5.98	3.20
Ho	mg/kg	0.775	0.991	0.951	1.66	0.712	1.03	1.22	0.650
Er	mg/kg	2.34	2.90	2.84	4.98	2.09	3.14	3.73	1.95
Tm	mg/kg	0.326	0.397	0.406	0.682	0.295	0.454	0.528	0.290
Yb	mg/kg	2.26	2.68	2.64	4.53	2.03	3.15	3.65	1.97
Lu	mg/kg	0.332	0.384	0.409	0.644	0.306	0.485	0.529	0.318
Hf	mg/kg	2.05	1.70	1.24	1.93	1.24	2.58	1.69	2.51
Ta	mg/kg	1.02	1.11	1.06	1.29	0.830	0.970	0.999	1.66
Hg	mg/kg	0.055	0.052	0.027	0.010	0.029	0.024	0.017	0.028
Tl	mg/kg	0.557	0.535	0.480	0.239	0.446	0.397	0.461	0.510
Pb	mg/kg	23.3	24.9	18.1	12.0	18.8	16.7	27.3	24.1
Bi	mg/kg	0.213	0.164	0.073	0.062	0.109	0.129	0.136	0.121
Th	mg/kg	10.2	17.3	9.72	10.1	7.07	10.2	21.6	9.79
U	mg/kg	2.49	2.24	1.55	1.08	1.10	1.64	2.44	1.70

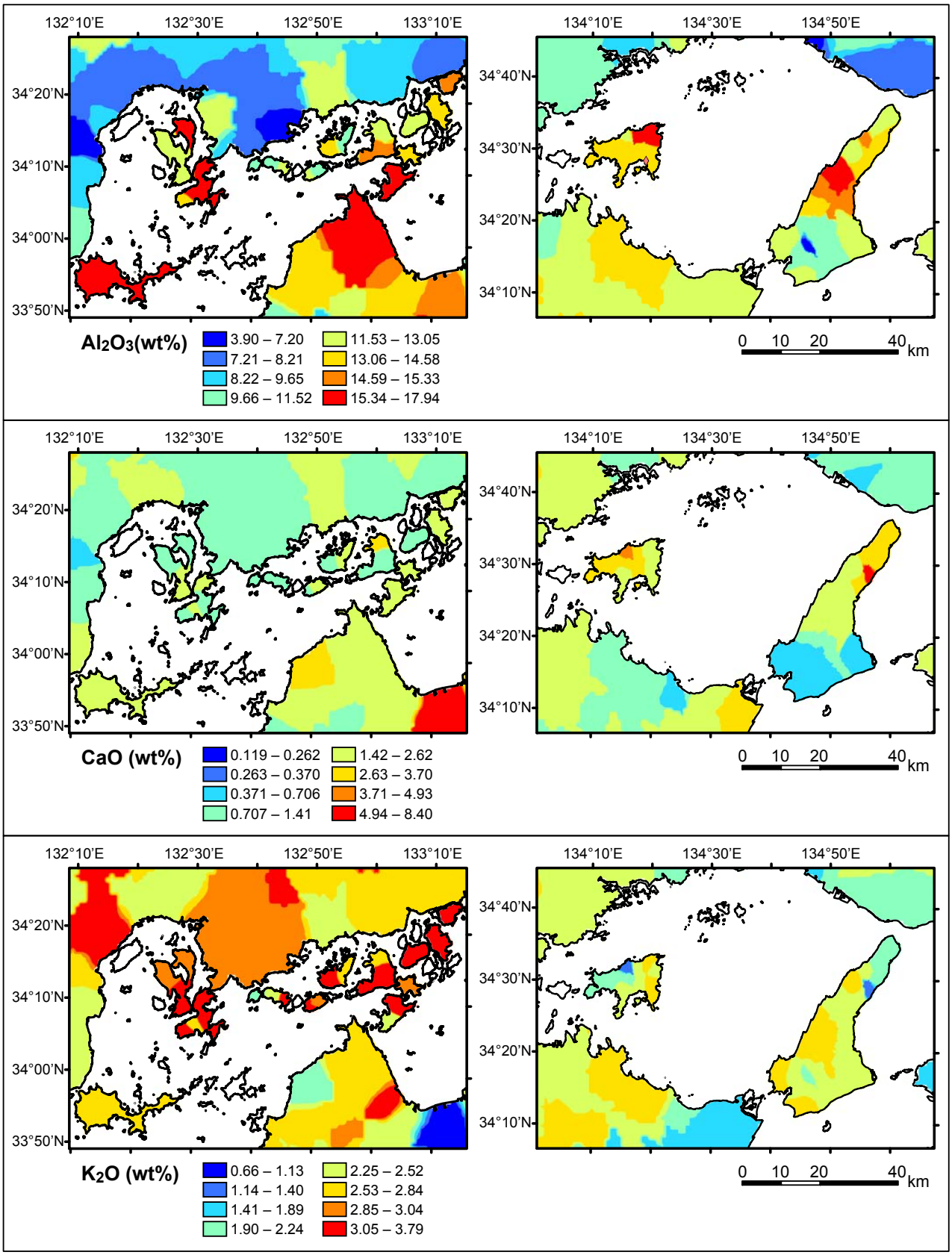

Fig. 6a Spatial distributions of elemental concentrations in the Seto Inland Sea region for Al_2O_3, CaO, K_2O, TiO_2, T-Fe_2O_3, Cr, Cu, Zn Cs, La, Yb, and Pb.

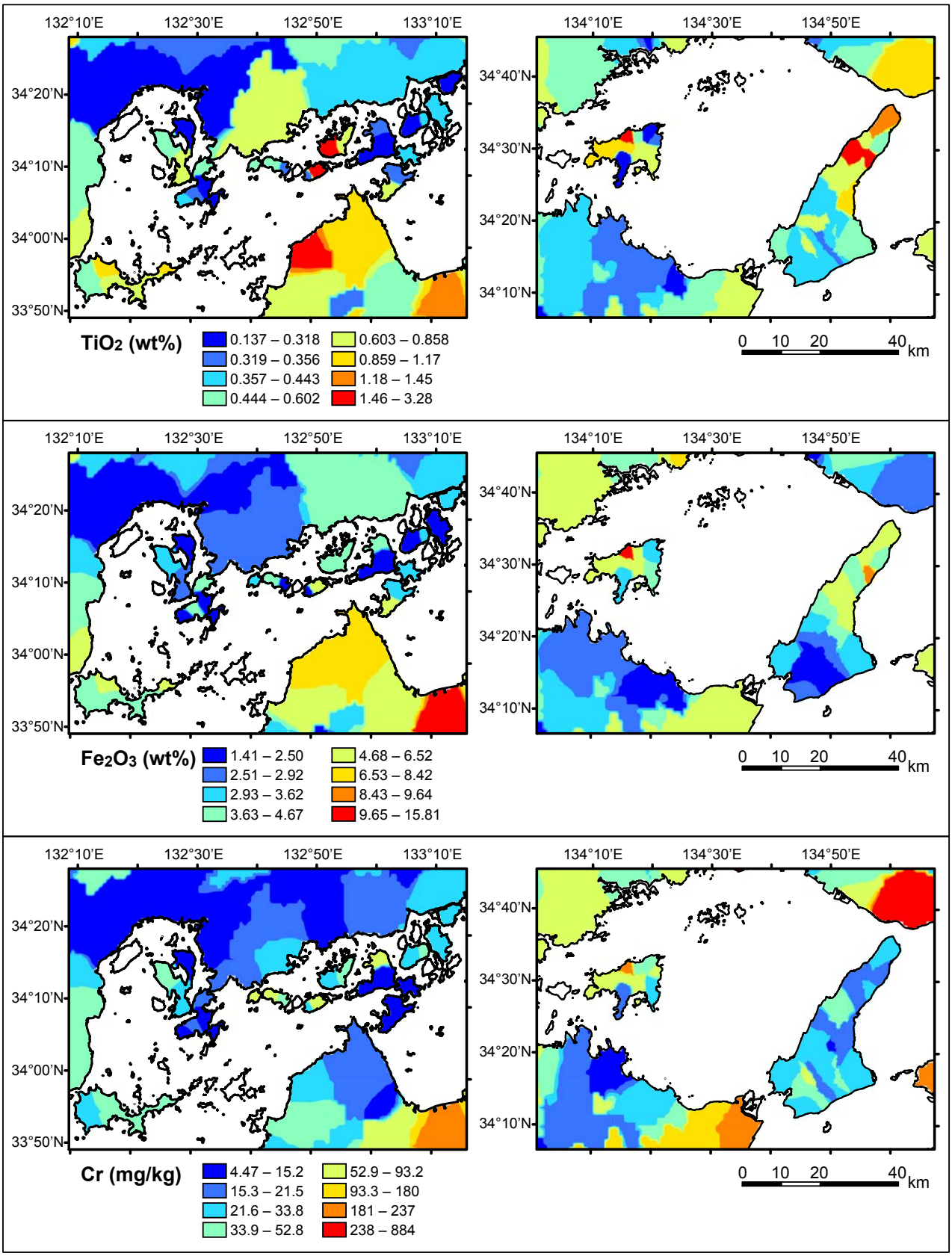

Fig. 6b Spatial distributions of elemental concentrations in the Seto Inland Sea region for Al_2O_3, CaO, K_2O, TiO_2, T-Fe_2O_3, Cr, Cu, Zn Cs, La, Yb, and Pb.

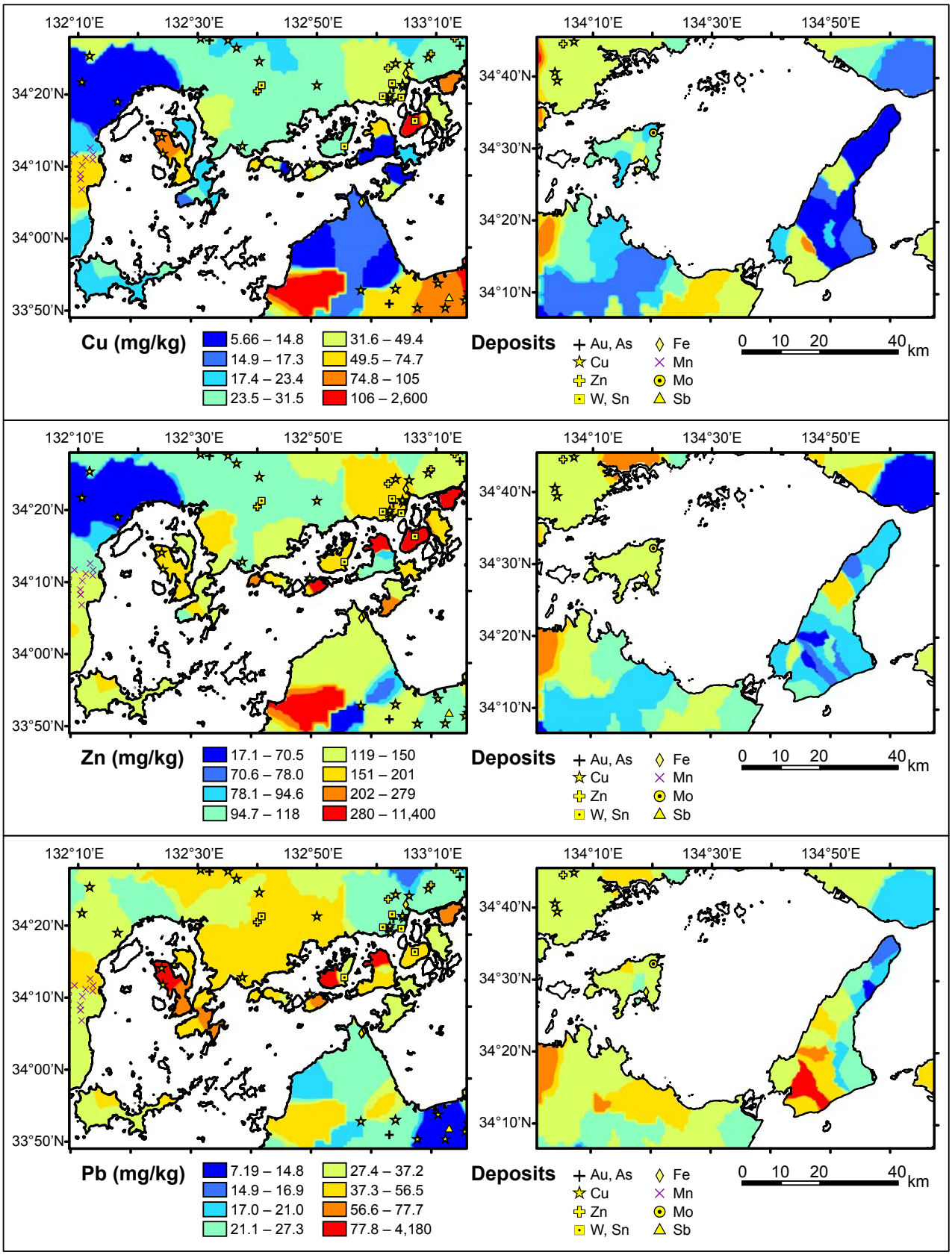

Fig. 6c Spatial distributions of elemental concentrations in the Seto Inland Sea region for Al_2O_3, CaO, K_2O, TiO_2, T-Fe_2O_3, Cr, Cu, Zn Cs, La, Yb, and Pb.

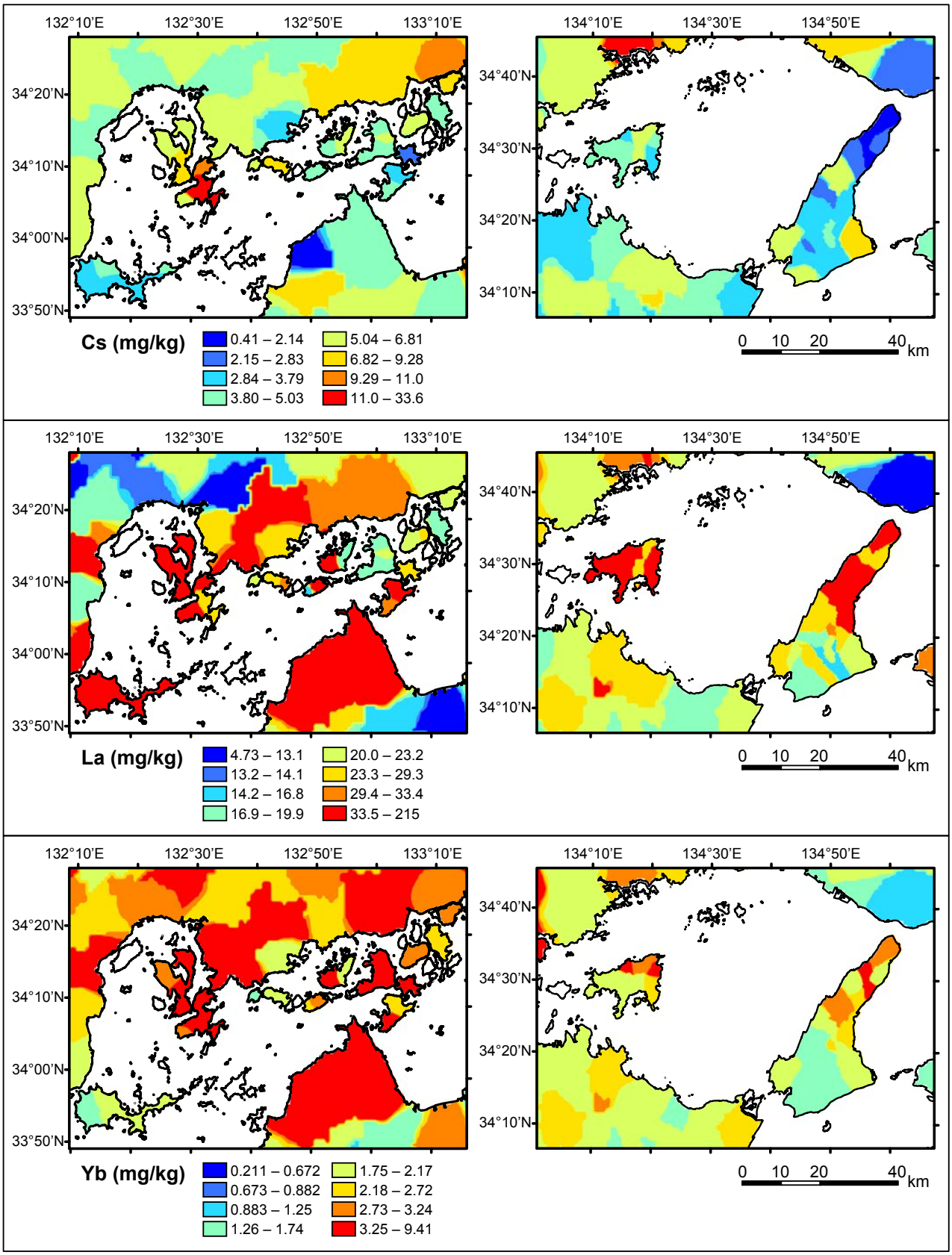

Fig. 6d Spatial distributions of elemental concentrations in the Seto Inland Sea region for Al_2O_3, CaO, K_2O, TiO_2, T-Fe_2O_3, Cr, Cu, Zn Cs, La, Yb, and Pb.

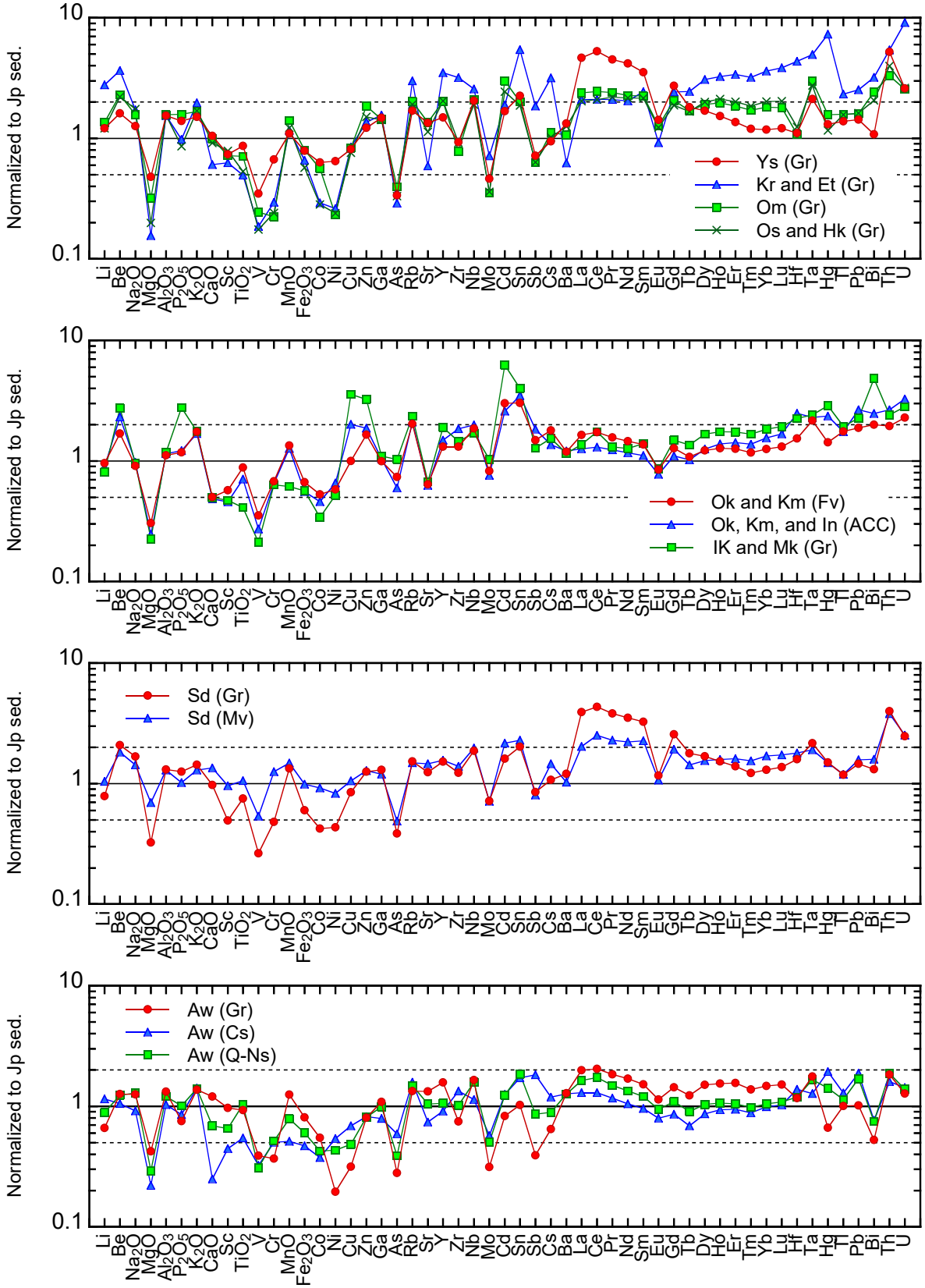

Fig. 7 Chemical compositions of stream sediments, classified with the parent lithology, normalized to the median concentrations of Japanese stream sediments, which is expressed as "Jp sed." (Imai *et al.*, 2004). The abbreviations Gr, ACC, Fv, Mv, Cs, and N-Qs indicate granitic rocks, sedimentary rocks of accretionary complexes, felsic and mafic volcanic rocks, Cretaceous sedimentary rocks (Izumi Group), and Neogene sediments, respectively.

mines (Fig. 6(c)) (e.g., Matsuura *et al.*, 2002). Although it is not shown in the figure, the highest Mo concentration (2.93 mg/kg) in sample Sd06 was likely caused by a Mo deposit located near the sampling site. However, the elevated concentrations of Cu, Zn, Mo, Cd, Sb, Hg, and Pb in stream sediments of Omishima Island (Om3) and Mukaishima Island (Mk1) are not fully explained by the metalliferous deposits. In Awajishima Island, high enrichments of Sn and Pb are found in the western part (AW09 and 10). Such spatial distributions were not recognized in the Shikoku Island (Fig. 6(c)). In addition, there are not any major mineral deposits in Awajishima Island. These samples may be polluted by human activity because elevated concentrations of metallic elements in Om3, Mk1, Aw09, and Aw10 are higher than their median values of stream sediments collected from urbanized areas such as Osaka City and Nagoya City (Ohta *et al.*, 2005).

4.6 Abundance patterns of elements in stream sediments normalized to Japanese stream sediments

Fig. 7 displays the median elemental concentrations of stream sediments normalized to the median concentrations of Japanese stream sediments (Imai *et al.*, 2004). Stream sediment samples were classified based on the dominant lithology in the watershed. Samples Kr3, Et1, Om3, and Sd5 were collected from irrigation channels that were covered with a small amount of sand. These samples were extremely enriched in Cr, Ni, Cu, Zn, Cd, Sn, Zr, Hf, REEs, Th, and U (Table 7) because heavy minerals and contaminated materials, which have a greater specific gravity, are concentrated in an unhampered channel during transport under a swift current. Therefore, these samples were not used for normalization and comparison.

Stream sediments derived from granitic rocks were enriched in Sn, light REEs, Th, and U, and depleted in MgO, CaO, Sc, TiO_2, V, Fe_2O_3, Cr, Co, Ni and Cu compared to Japanese stream sediments (see samples with the abbreviation Gr in Fig. 7). Stream sediments in Kurahashijima Island (Kr1, Kr2, and Kr4) and Etajima Island (Et3) were highly abundant in Li, Be, Rb, Y, Zr, Nb, Sn, Cs, heavy REEs (Dy–Lu), Hf, Ta, Th, and U, poor in CaO, Sr, and Ba, and characterized by a large negative Eu anomaly (Kr and Et (Gr) in Fig. 7). These features found in the abundance pattern are likely due to the accumulation of xenotime and zircon and a small amount of plagioclase. In contrast, sediments in Yashirojima Island and Shodoshima Island had extremely high concentrations of light REEs (La–Sm) and Th, relatively high concentrations of MgO, V, Cr, Co, and Ni, and a large negative Eu anomaly (Ys (Gr) and Sd (Gr) in Fig. 7). The extreme enrichment in light REEs relative to heavy REEs in Yashirojima Island is likely due to the accumulation of rare earth minerals, as described previously (Minakawa *et al.*, 2001). Yashirojima Island is underlain by Ryoke biotite-hornblende granodiorite, and the other islands are underlain by Hiroshima biotite- or biotite-hornblende granite and partly by Hiroshima hornblende granodiorite (Igi *et al.*, 1987; Matsuura *et al.*, 2002; Miyazaki *et al.*, 2016; Yamada *et al.*, 1986). The higher concentrations of MgO, V, Cr, and Ni indicate that stream sediments in Yashirojima Island are relatively enriched in biotite and hornblende compared to the other islands.

Stream sediments derived from felsic volcanic rocks and sedimentary rocks of accretionary complexes had similar abundance patterns (see the "Ok and Km (Fv)" and the "Ok, Km, and In (ACC)" in Fig. 7). Their abundance patterns also resembled that of sediments originating from granitic rocks, except for P_2O_5, Cu, Zn, Cd, and Bi, which were strongly influenced by mineral deposits and anthropogenic contamination.

In Shodoshima Island, sediments originating from mafic volcanic rocks (Sd (Mv) in Fig. 7) were abundant in MgO, Sc, TiO_2, V, Fe_2O_3, Co, and Ni, and less abundant in light REEs compared to those from granitic rocks (Sd (Gr) in Fig. 7). However, the abundances of the remaining elements were comparable. Almost all samples in Shodoshima Island were collected from an area underlain by granitic rocks, although granitic rocks are the dominant lithology for only two samples (Table 2). Therefore, the geochemistry of stream sediments in Shodoshima Island is can be explained with a simple mixture of granitic and mafic volcanic rocks.

Stream sediments originating from granitic rocks in Awajishima Island were heavily depleted in Cr, Ni, Cu, As, Rb, Mo, Cd, Sn, Sb, Hg, Pb, and Bi, which was related to local mineral deposits and anthropogenic contamination (Aw (Gr) in Fig. 7). The Izumi Group provides systematically lower concentrations of MgO, CaO, Sc, TiO_2, MnO, Fe_2O_3, and Sr to stream sediments than granitic rocks (Aw (Cs) in Fig. 7). The low concentrations of these elements could have been related to the lower abundances of mafic minerals in the Izumi Group. Except for elements related to mineral deposits, contamination, and mafic minerals, the abundance pattern of elements in stream sediments derived from the Izumi Group resembles that from granitic rocks, although their REE concentrations are systematically low. This relationship suggests that the Izumi Group may have originated from Ryoke granitic rocks. Stream sediments originating from Neogene sediments in the northern part of Awajishima Island had intermediate elemental compositions between the granitic rocks and Izumi Group (Aw (Q-Ns) in Fig. 7).

5. Summary

The straightforward and rapid determination of 53 elements in stream sediments by ICP-AES, ICP-MS, and AAS was evaluated for geochemical mapping of isolated islands. Stream sediment samples were decomposed with HF, HNO_3, and $HClO_4$ at 125°C for 2 h and further at 145°C during 1 h prior to 51 elemental measurements. The decomposition at 125–145 °C for 3 h improved the determination of TiO_2, REEs, Nb, Zr, Ta, and Hf included

in refractory minerals. However, the HF-HNO_3-$HClO_4$ digestion cannot completely decompose the heavy mineral fraction, including zircon ($ZrSiO_4$), the analytical values of Zr and Hf in stream sediments should be used as a guide only. Sample was digested using a mixed acid solution with $KMnO_4$ at 120°C for 20 min for As determination, a different procedure from the analysis described above for the 51 other elements. As concentrations decreased significantly with increasing decomposition temperature and time and/or decomposing samples without using $KMnO_4$. The mercury concentrations in sediments were determined using an AAS analyzer after heating the 50 mg samples and vaporizing Hg. Analytical data for geochemical reference materials were in agreement with the certified and recommended values. The RSDs of measured elements in geochemical reference materials were 1–5% for most elements and 10% for Hg and elements having low concentrations. Thus, it was confirmed that the precision and accuracy of this rapid and straightforward analysis for geochemical mapping were satisfactory.

The geochemical features of stream sediments in the isolated islands of the Seto Inland Sea were strongly influenced by the parent lithology distributed in their watersheds. Sediments were enriched in Na_2O, Al_2O_3, K_2O, Be, Rb, Nb, REEs, Ta, Th, and U in the sediments of isolated islands with widely underlain granitic rocks. Extreme enrichment in REEs, Nb, Ta and Th in stream sediments of Yashirojima Island, Kurahashijima Island, Etajima Island and Shodoshima Island were likely due to the accumulation of rare earth minerals. MgO, TiO_2, V, Cr, MnO, Fe_2O_3, Ni, and Co were abundant in the sediments of Shodoshima Island whose central part is occupied with mafic volcanic rocks. Small scale Cu, W, and Mo mines elevated concentrations of Cu, Zn, As, Mo, Cd, Sn, Sb, Hg, Pb, and Bi in Etajima Island, Osaki-kamijima Island, Ikuchishima Island, and Shodoshima Island. However, high concentrations of Cu, Zn, Mo, Cd, Sb, and Pb in Omishima Island and Mukaishima Island, and Cu, Cd, Sb, and Hg in Awajishima Island were likely due to anthropogenic activity because any influence of metalliferous deposits could not be found.

Acknowledgement

I express my appreciation to Dr. T. Okai for his useful suggestions, which helped to improve an earlier version of this manuscript.

References

Cicchella, D., De Vivo, B., Lima, A., Albanese, S. and Fedele, L. (2008) Urban geochemical mapping in the Campania region (Italy). *Geochemistry: Exploration Environment Analysis*, **8**, 19–29.

De Vos, W., Tarvainen, T., Salminen, R., Reeder, S., De Vivo, B., Demetriades, A., Pirc, S., Batista, M. J., Marsina, K., Ottesen, R.-T., O'Connor, P. J., Bidovec, M., Lima, A., Siewers, U., Smith, B., Taylor, H., Shaw, R., Salpeteur, I., Gregorauskiene, V., Halamic, J., Slaninka, I., Lax, K., Gravesen, P., Birke, M., Breward, N., Ander, E. L., Jordan, G., Duris, M., Klein, P., Locutura, J., Bel-lan, A., Pasieczna, A., Lis, J., Mazreku, A., Gilucis, A., Heitzmann, P., Klaver, G. and Petersell, V. (2006) *Geochemical atlas of Europe. Part 2 - Interpretation of Geochemical Maps, Additional Tables, Figures, Maps, and Related Publications*. Geological Survey of Finland, Espoo, Finland, 692p.

Geological Survey of Japan, AIST (ed.) (2015) *Seamless digital geological map of Japan 1: 200,000. May 29, 2015 version*. Research Information Database DB084, Geological Survey of Japan, National Institute of Advanced Industrial Science and Technology.

Geological Survey of Japan, AIST (2017) GSJ Geochemical Reference samples. Geological Survey of Japan, Avaiable online: https://gbank.gsj.jp/geostandards/ (accessed 2017-6-20).

Howarth, R. J. and Thornton, I. (1983) Regional Geochemical Mapping and its Appli cation to Environmental Studies. *In* Thornton, I., ed., *Applied Environmental Geochemistry*, Academic Press, London, 41–73.

Igi, S., Murakami, N. and Okubo, M. (1987) *Regional Geology of Japan. Part 7 (CHUGOKU)*. Kyoritsu Shuppan Co., 304p (in Japanese).

Imai, N. (1987) Multielement analysis of stream sediment by ICP-AES. *Bunseki Kagaku*, **36**, T41–T45 (in Japanese with English abstract).

Imai, N. (1990) Multielement analysis of rocks with the use of geological certified reference material by inductively coupled plasma mass spectrometry. *Anal. Sci*., **6**, 389–395.

Imai, N. (2010) Investigation of the distribution of elements of the whole of Japan and their applications - Geochemical map of land and sea of Japan -. *Synthesiology*, **3**, 281–291.

Imai, N., Terashima, S., Itoh, S. and Ando, A. (1995) 1994 compilation of analytical data for minor and trace-elements in 17 GSJ geochemical reference samples, igneous rock series. *Geostand. Newsl*., **19**, 135–213.

Imai, N., Terashima, S., Itoh, S. and Ando, A. (1996) 1996 compilation of analytical data on nine GSJ geochemical reference samples, "Sedimentary rock series". *Geostand. Newsl*., **20**, 165–216.

Imai, N., Terashima, S., Ohta, A., Mikoshiba, M., Okai, T., Tachibana, Y., Togashi, S., Matsuhisa, Y., Kanai, Y., Kamioka, H. and Taniguchi, M. (2004) Geochemical map of Japan. Geological Survey of Japan, AIST, 209p. (Database available from https://gbank.gsj.jp/geochemmap/, accessed 2017-6-20).

Imai, N., Terashima, S., Ohta, A., Mikoshiba, M., Okai, T., Tachibana, Y., Togashi, S., Matsuhisa, Y., Kanai, Y. and Kamioka, H. (2010) Geochemical Map of Sea and Land of Japan. Geological Survey of Japan, AIST, Tsukuba, 207p. (Database available from https://

gbank.gsj.jp/geochemmap/, accessed 2017-6-20).

Imai, N., Okai, T., Ohta, A., Mikoshiba (Ujiie), M., Kanai, Y., Kubota, R., Tachibana, Y., Terashima, S., Ikehara, K., Katayama, H. and Noda, A. (2015) Geochemical Map of Kanto Region. Geological Survey of Japan, AIST, Tsukuba, 217p. (Database available from https://gbank.gsj.jp/geochemmap/, accessed 2017-6-20).

Johnson, C. C. and Ander, E. L. (2008) Urban geochemical mapping studies: how and why we do them. *Environ. Geochem. Health*, **30**, 511–530.

Kurimoto, C., Makimoto, H., Yoshida, F., Takahashi, Y. and Komazawa, M. (1998) *Geological Map of Japan 1:200,000, Wakayama*. Geological Survey of Japan.

Makimoto, H., Toshimitsu, S., Takahashi, Y., Mizuno, K., Komazawa, M. and Shichi, R. (1995) *Geological Map of Japan 1:200,000, Tokushima (2nd edition)*. Geological Survey of Japan.

Matsuura, H., Kurimoto, C., Yoshida, F., Saito, Y., Makimoto, H., Toshimitsu, S., Iwaya, T., Komazawa, M. and Hiroshima, T. (2002) *Geological Map of Japan 1: 200,000, Okayama and Marugame*. Geological Survey of Japan.

Minakawa, T., Funakoshi, N. and Morioka, H. (2001) Chemical properties of allanite from the Ryoke and Hirosima granite pegmatites in Shikoku, Japan. *Men. Fac. Sci. Ehime Univ.*, **7**, 1–13.

Miyazaki, K., Wakita, K., Miyashita, Y., Mizuno, K., Takahashi, M., Noda, A., Toshimitsu, S., Sumii, T., Ohno, T., Nawa, K. and Miyakawa, A. (2016) *Geological Map of Japan 1:200,000, Matsuyama (2nd edition)*. Geological Survey of Japan.

Ohta, A., Imai, N., Tachibana, Y. and Ikehara, K. (2017) Statistical Analysis of the Spatial Distribution of Multi-Elements in an Island Arc Region: Complicating Factors and Transfer by Water Currents. *Water*, **9**, 37: 31–26.

Ohta, A., Imai, N., Terashima, S., Tachibana, Y., Ikehara, K. and Katayama, H. (2015) Elemental distribution of surface sediments around Oki Trough including adjacent terrestrial area: Strong impact of Japan Sea Proper Water on silty and clayey sediments. *Bull. Geol. Surv. Japan*, **66**, 81–101.

Ohta, A., Imai, N., Terashima, S., Tachibana, Y., Ikehara, K., Katayama, H. and Noda, A. (2010) Factors controlling regional spatial distribution of 53 elements in coastal sea sediments in northern Japan: Comparison of geochemical data derived from stream and marine sediments. *Appl. Geochem.*, **25**, 357–376.

Ohta, A., Imai, N., Terashima, S. and Tachibana, Y. (2005) Application of multi-element statistical analysis for regional geochemical mapping in Central Japan. *Appl. Geochem.*, **20**, 1017–1037.

Ohta, A., Imai, N., Terashima, S., Tachibana, Y., Ikehara, K. and Nakajima, T. (2004) Geochemical mapping in Hokuriku, Japan: influence of surface geology, mineral occurrences and mass movement from terrestrial to marine environments. *Appl. Geochem.,* **19**, 1453–1469.

Okai, T., Terashima, S. and Imai, N. (2002) Collaborative analysis of GSJ geochemical reference materials JCu-1 (copper ore) and JZn-1 (zinc ore). *Bunseki Kagaku*, **51**, 973–977 (in Japanese with English abstract).

Reimann, C., Siewers, U., Tarvainen, T., Bityukova, L., Eriksson, J., Gilucis, A., Gregorauskiene, V., Lukashev, V., Matinian, N. and Pasieczna, A. (2003) *Agricultural Soils in Northern Europe: A Geochemical Atlas*. E. Schweizerbart'sche Verlagsbuchhandlung, Stuttgart, Germanyp.

Salminen, R., Batista, M. J., Bidovec, M., Demetriades, A., B., D. V., De Vos, W., Duris, M., Gilucis, A., Gregorauskiene, V., Halamic, J., Heitzmann, P., Lima, A., Jordan, G., Klaver, G., Klein, P., Lis, J., Locutura, J., Marsina, K., Mazreku, A., O'Connor, P. J., Olsson, S. Å., Ottesen, R.-T., Petersell, V., Plant, J. A., Reeder, S., Salpeteur, I., Sandström, H., Siewers, U., Steenfelt, A. and Tarvainen, T. (2005) *Geochemical atlas of Europe. Part 1 - Background Information, Methodology and Maps*. Geological Survey of Finland, Espoo, Finland, 526p.

Terashima, S. (1976) The determination of arsenic in rocks, sediments and minerals by arsine generation and atomic absorption spectrometry. *Anal. Chim. Acta*, **86**, 43–51.

Terashima, S. (1984) Determination of arsenic and antimony in geological-materials by automated hydride generation and electrothermal atomic-absorption spectrometry. *Bunseki Kagaku*, **33**, 561–563 (in Japanese with English abstract).

Terashima, S. (1997) Determination of molybdenum in fifty three geochemical reference materials by flameless atomic absorption spectrometry. *Geostand. Newsl.*, **21**, 93–96.

Terashima, S., Imai, N., Taniguchi, M., Okai, T. and Nishimura, A. (2002a) The preparation and preliminary characterisation of four new Geological Survey of Japan geochemical reference materials: Soils, JSO-1 and JSO-2; and marine sediments, JMS-1 and JMS-2. *Geostand. Newsl.*, **26**, 85–94.

Terashima, S., Okai, T. and Imai, N. (2002b) Determination of bismuth in fifty geological reference materials by AAS. *Bunseki Kagaku*, **51**, 317–322 (in Japanese with English abstract).

Terashima, S., Taniguchi, M., Mikoshiba, M. and Imai, N. (1998) Preparation of two new GSJ geochemical reference materials: Basalt JB-1b and coal fly ash JCFA-1. *Geostand. Newsl.*, **22**, 113–117.

Terashima, S., Usui, A. and Imai, N. (1995) Two new GSJ geochemical reference samples: Syenite JSy-1 and manganese-nodule JMn-1. *Geostand. Newsl.*, **19**, 221–229.

Thornton, I., Farago, M. E., Thums, C. R., Parrish, R. R., McGill, R. A. R., Breward, N., Fortey, N. J., Simpson, P., Young, S. D., Tye, A. M., Crout, N. M. J., Hough, R.

L. and Watt, J. (2008) Urban geochemistry: research strategies to assist risk assessment and remediation of brownfield sites in urban areas. *Environ. Geochem. Health*, **30**, 565–576.

Weaver, T. A., Broxton, D. E., Bolivar, S. L. and Freeman, S. H. (1983) *The Geochemical Atlas of Alaska: Compiled by the Geochemistry Group, Earth Sciences Division, Los Alamos National Laboratory*. GJBX-32(83), Los Alamos, 141p.

Webb, J. S., Thornton, I., Thompson, M., Howarth, R. J. and Lowenstein, P. L. (1978) *The Wolfson Geochemical Atlas of England and Wales*. Clarendon Press, Oxford, 69p.

Yamada, N., Higashimoto, S., Mizuno, K., Hiroshima, T. and Suda, Y. (1986) *Geological Map of Japan 1:200,000, Hiroshima*. Geological Survey of Japan.

Recieved June 30, 2017
Accepted December 4, 2017

日本離島域の地球化学図作成に向けた河川堆積物中の簡易・迅速多元素分析に対する評価
―瀬戸内海島嶼域―

太田充恒

要　旨

離島域の地球化学図作成に向けて，ICP発光分析，ICP質量分析，原子吸光分析を用いて測定した河川堆積物中の 53 元素の迅速かつ簡易分析法の評価を行った．0.1 g の試料をフッ酸・硝酸・過塩素酸を用いて125℃下で 2 時間分解後，更に145℃下で 1 時間の追加分解を加えることで，難溶性鉱物に多く含まれる元素の定量性の改善を試みた．結果，希土類元素，Nb，Taについては 5–15%，Zr，Hfについては 30%の改善結果を得た．ヒ素の分析においては，0.1 g の試料を酸化剤である過マンガン酸カリウムを添加した混酸を用いて 120℃下で 20 分間の分解を行った．酸化剤を添加しない場合や長時間の分解を行った場合，地球化学標準物質中のヒ素の濃度は低下した．しかし，河川堆積物試料中のヒ素濃度は過マンガン酸カリウムの添加や分解時間に関係なくほぼ同じ値を示した．水銀分析は，前処理なしに試料約 50 mgを加熱・気化させた水銀を原子吸光法で測定した．ICP発光分析，ICP質量分析，原子吸光分析を用いて測定した地球化学標準物質中の 53 元素の濃度は推奨値と良く一致した．これらの結果から，地球化学図作成のための簡易・迅速分析は十分な精度を持っていると結論づけられる．

瀬戸内海島嶼の河川堆積物の地球化学的特徴は，その河川流域に分布する母岩に強く影響されていた．Na_2O，Al_2O_3，K_2O，Be，Rb，Nb，REEs，Ta，Tl，Th，Uなどは花崗岩が広く分布する離島から採取した堆積物に多く含まれていた．一方，MgO，TiO_2，V，Cr，MnO，Fe_2O_3，Ni，Coは塩基性火山岩が噴出した小豆島の堆積物に多く含まれていた．鉱床や人為汚染に関係していた河川堆積物にはCu，Zn，As，Mo，Cd，Sn，Sb，Hg，Pb，Biの極端な濃集が認められた．